MAX-PLANCK-GESELLSCHAFT

Modeling Cancer Ecology

examples of the public goods game

Philipp Altrock

Max Planck Institute for Evolutionary Biology

philipp.altrock@gmail.com

@evlosci

thanks

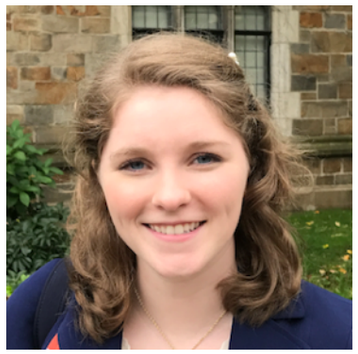

Meghan Ferrall-Fairbanks, PhD
(University of Florida)

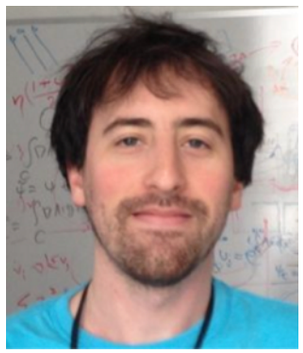

Greg J. Kimmel, PhD
(formerly Moffitt)

Philip Gerlee, PhD
(Chalmers)

Brian Johnson, BSc
(UCSD)

Noemi Andor, PhD
(Moffitt)

COIs

KITE Pharma (Gilead): research funding

CRISPR Therapeutics: consulting

outline

- Evolution and Ecology of Cancer
- Clonal interactions and the heterogeneity
- Public Goods Game among Cells
- Stochasticity, Assortment, Space
- Conclusions and Outlook

cancer is a complex *evolving* system

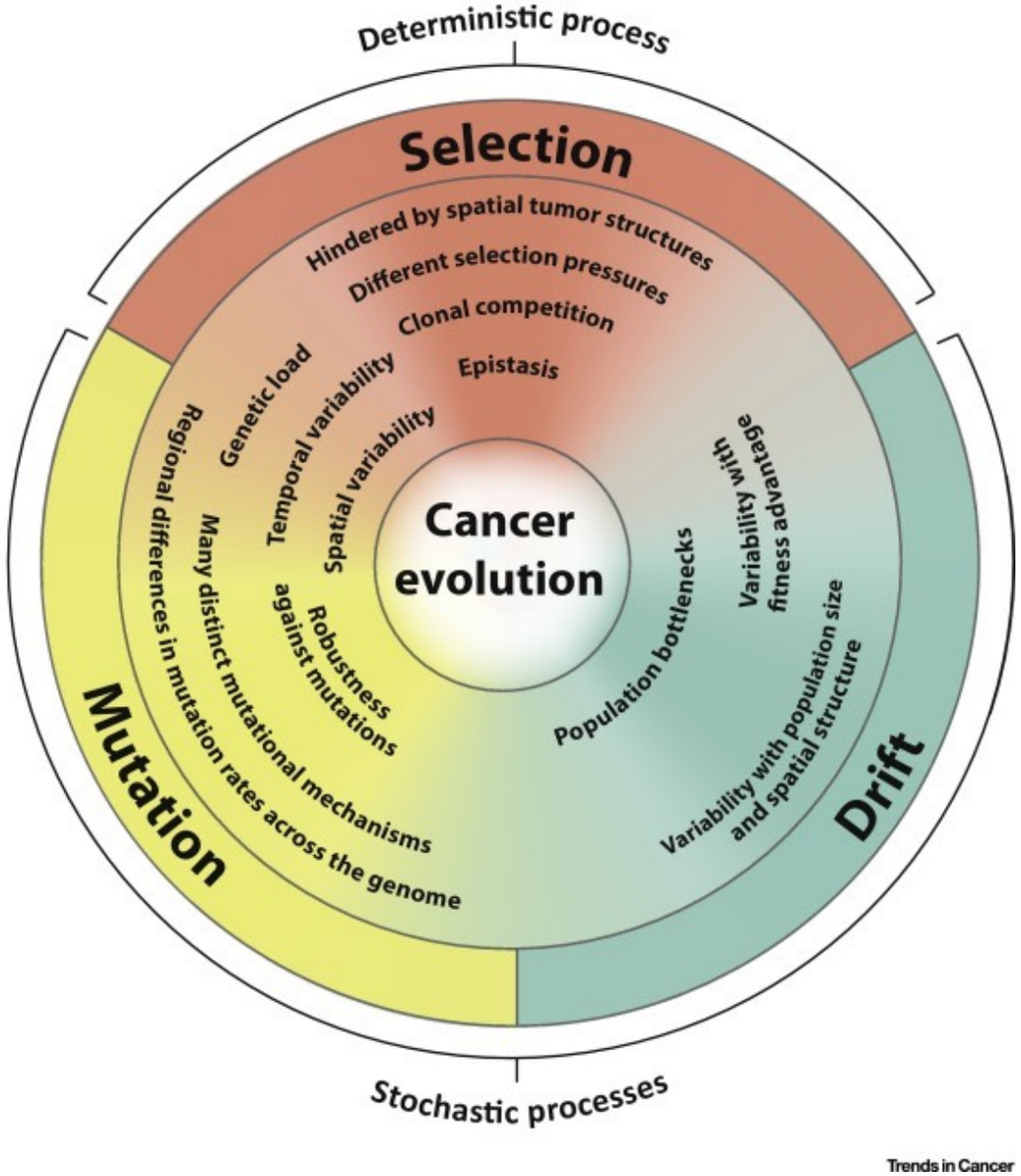

We seek to understand selection in cancer cell populations.

Lipinski *et al.*, Trends in Cancer 2016

modeling cancer dynamics

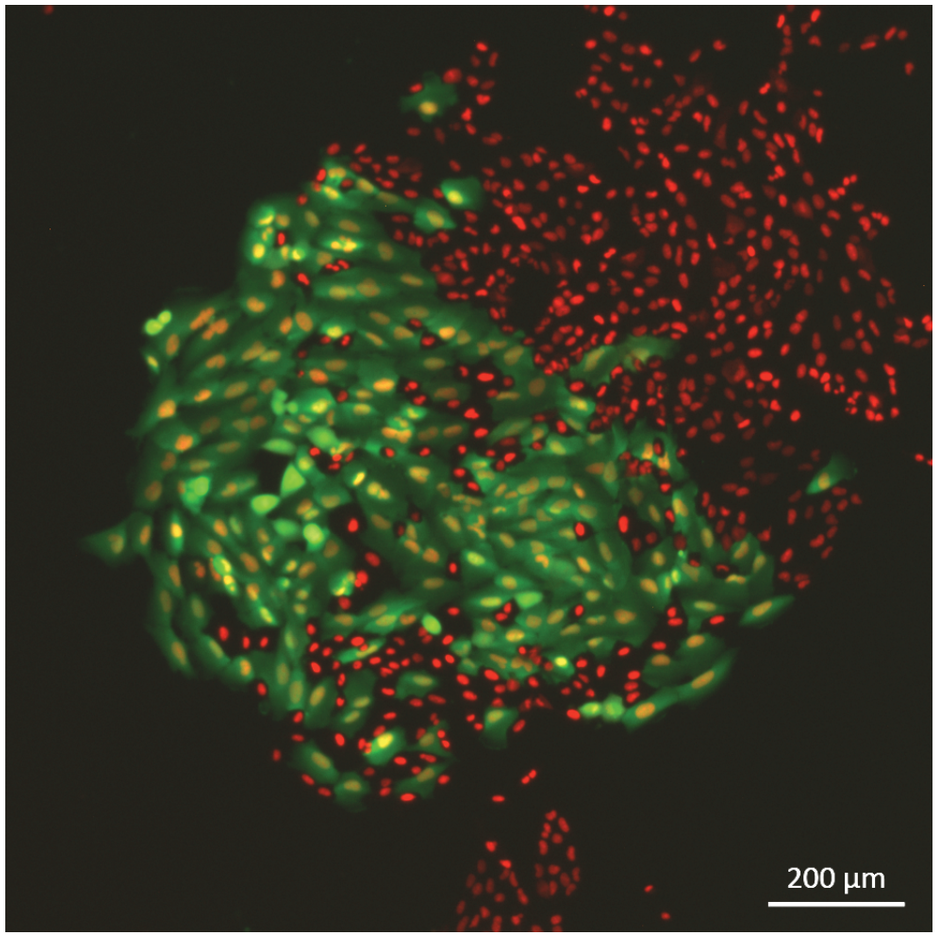

Image of live fluorescent colony formed after a selection experiment
Human breast cancer cell lines: SUM159/MDA231

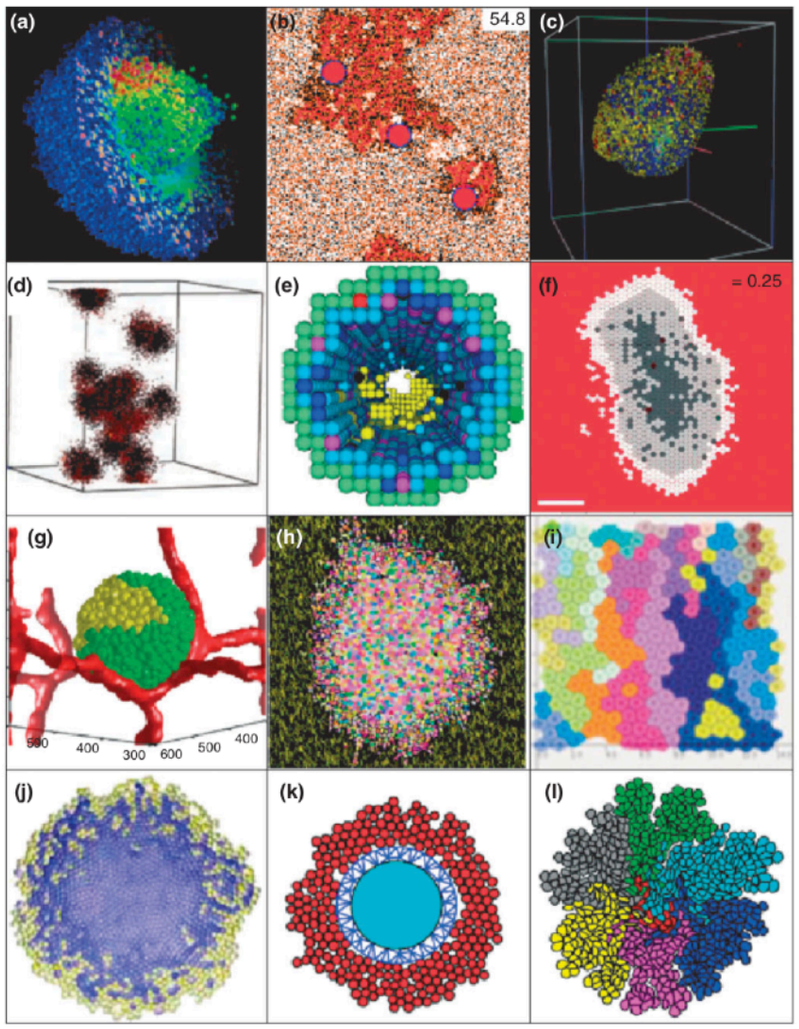

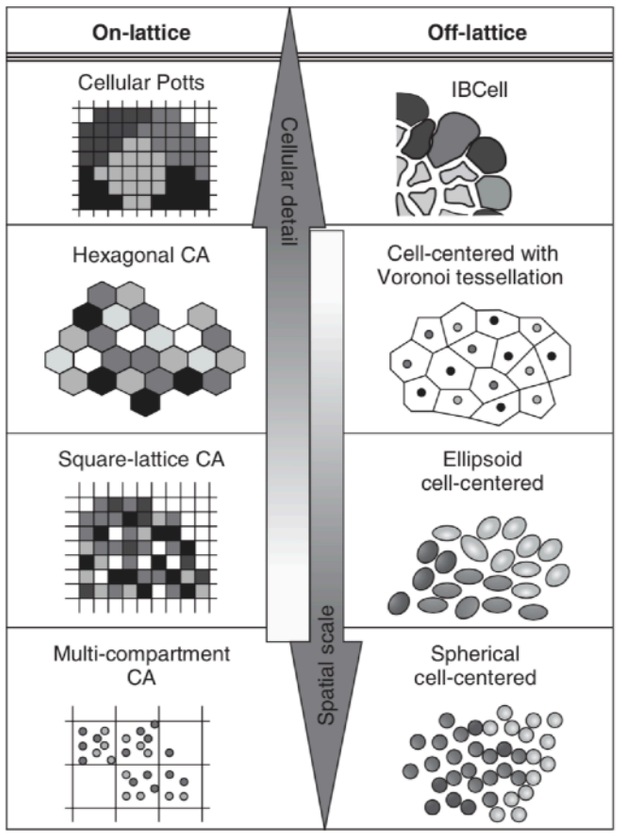

FIGURE 1 | Reciprocal relation between the number of cells handled by the models and the level of included cellular details. In each class (on-lattice and off-lattice), the models complexity rises from cells represented by single points to fully deformable bodies.

Miroshnychenko, *et al.* Nature Ecology & Evolution 2021, Rejniak & Anderson, Interface focus 2010

processes and mechanisms in cancer evolution: stochastic processes

Branching processes, Moran process with selection

<u>Branching process in cancer</u>:
work by Bozic, Durrett, Antal, Tomasetti

<u>Evolutionary Moran process</u>:
in <u>cancer</u>: work by Michor, Foo

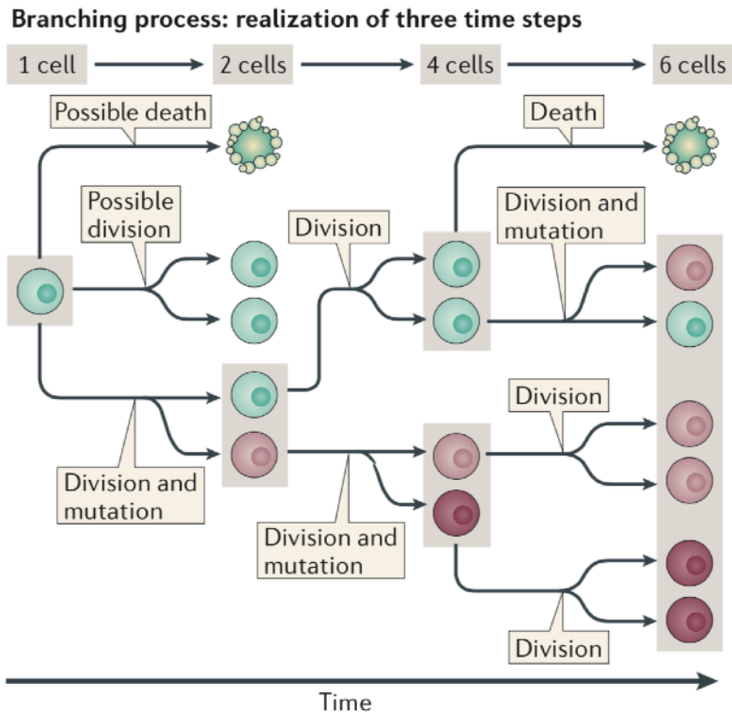

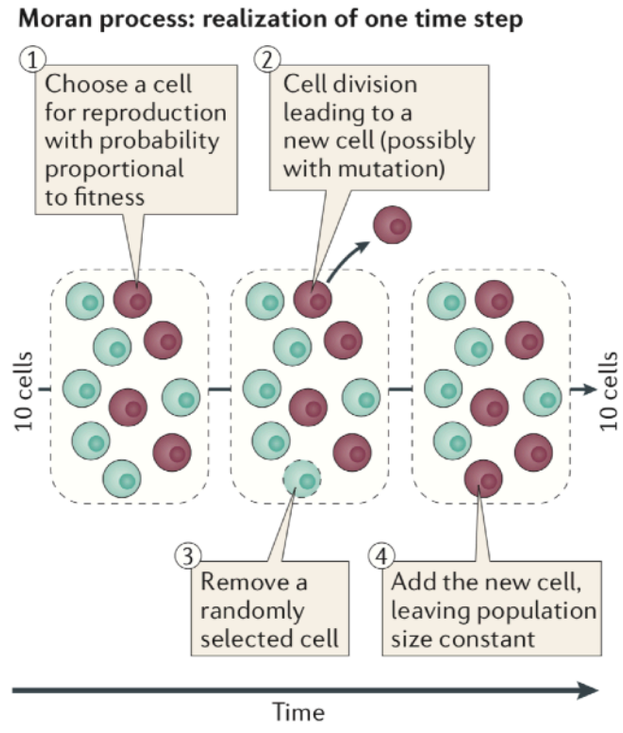

Altrock, Liu & Michor, Nature Reviews Cancer 2015

processes and mechanisms in cancer evolution: nonlinear dynamics

Nonlinear dynamics, reaction-advection-diffusion systems

Work by Anderson, Maini & many others
Kimmel, Dane, Heiser, Altrock & Andor, Cancer Res. 2020

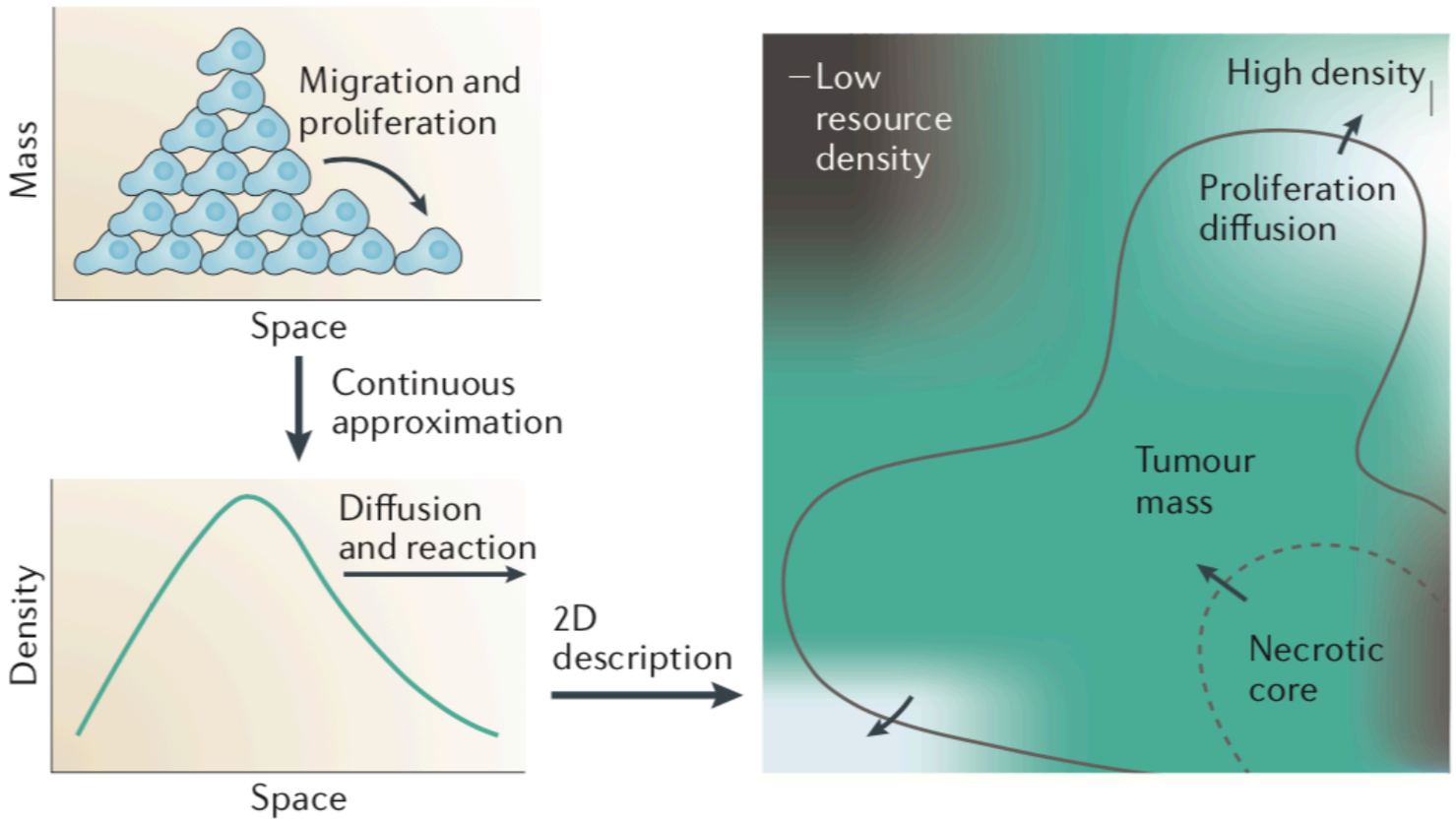

cell movement (m) and growth neighborhood (ω) can lead to different growth curves

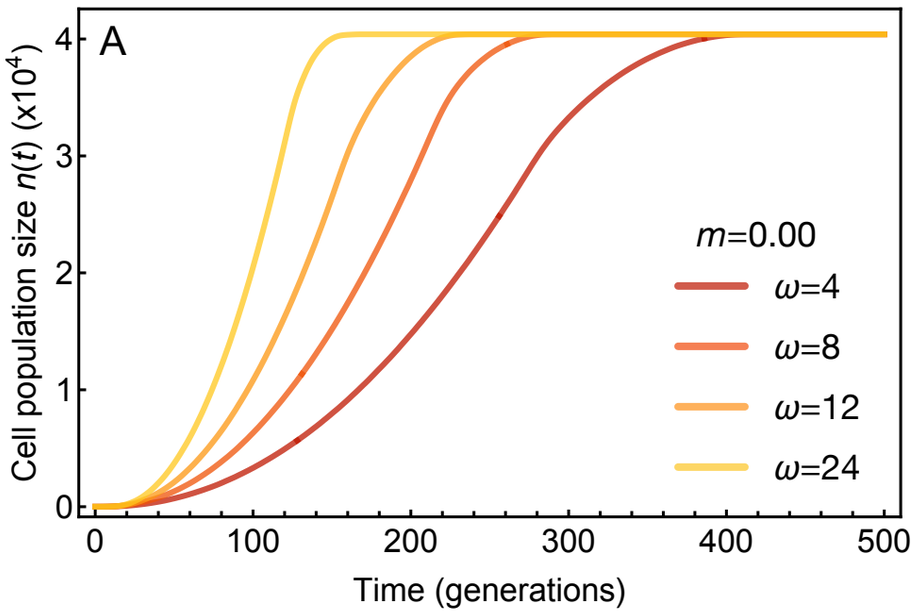

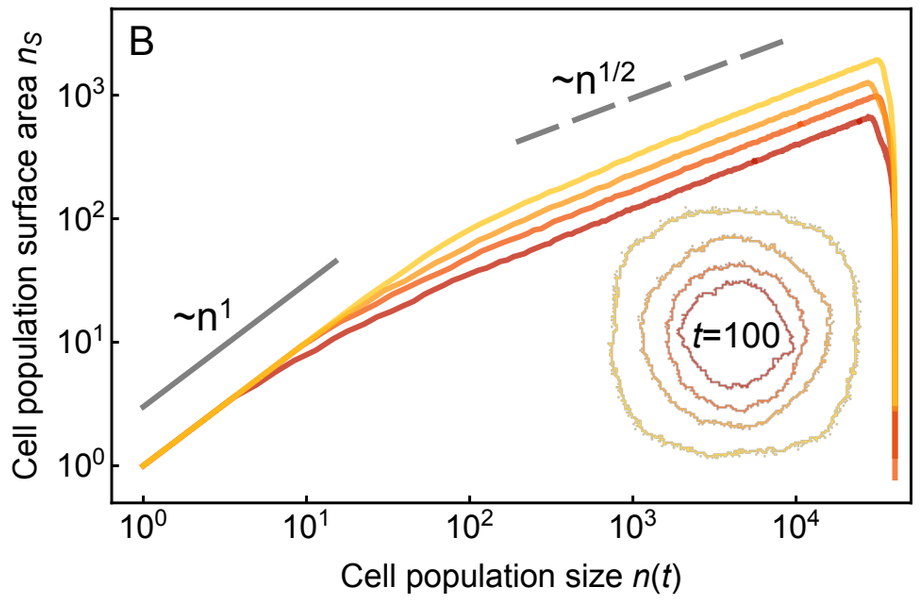

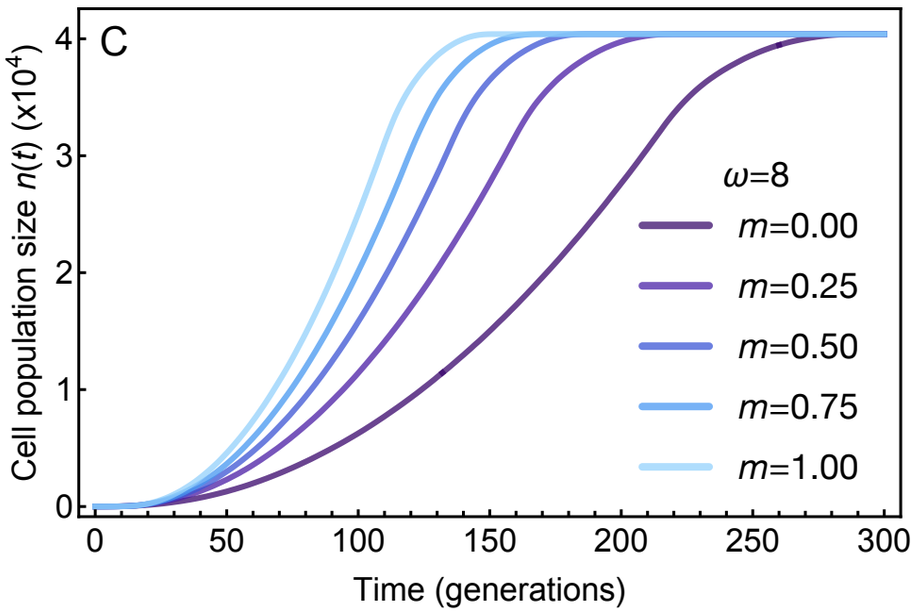

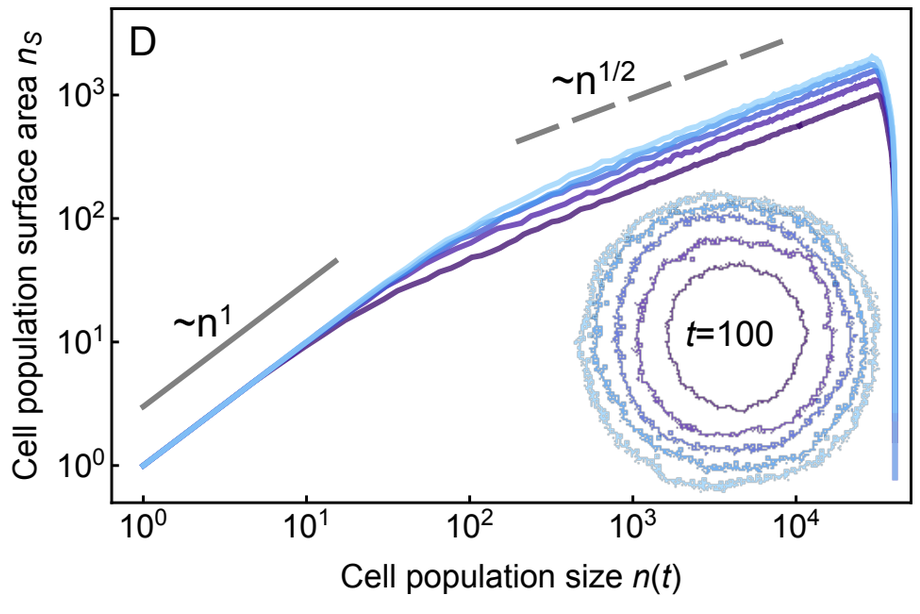

Kimmel *et al.*, bioRXiv.org 2021

cancer evolution leads to heterogeneity, e.g., due to clonal interference or ecological interactions

"at the time of clinical diagnosis, the majority of human tumors display startling heterogeneity in many morphological and physiological features, such as expression of cell surface receptors, proliferative and angiogenic potential"

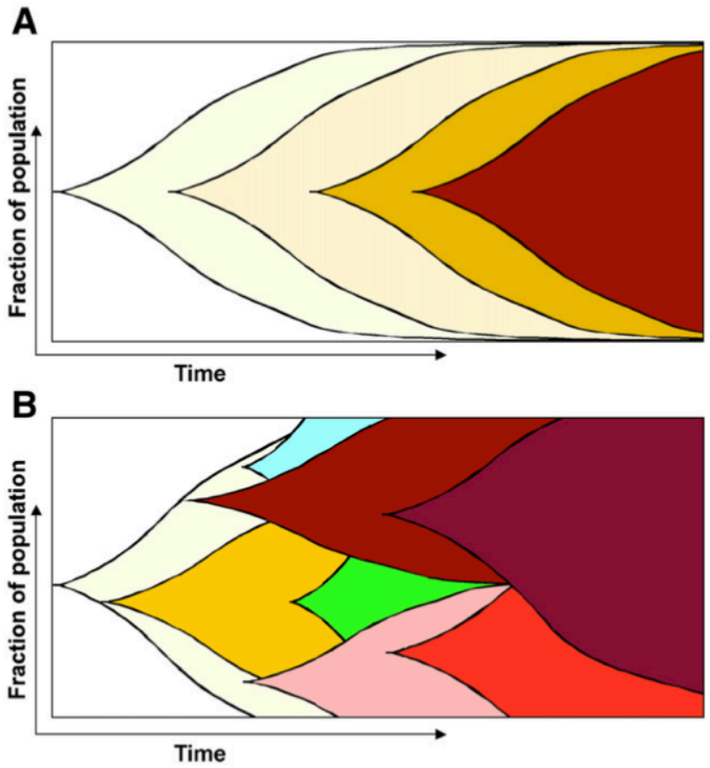

Fig. 1. Schematic view of monoclonal and multiclonal models of tumor progression. Increasing color intensity correlates with tumor progression, whereas different colors reflect different clones. (A) Traditional, linear model of clonal succession, where progressive mutations in oncogenes and tumor suppressor genes drive linear succession of rounds of clonal expansion, manifested as tumor progression. (B) Multi-clonal model of tumor progression: although all cells in tumors originate from a single initiated cell, the evolution of the tumor is more "messy", with genetically divergent tumor clones co-existing within tumors for substantial periods of time. The population sizes and characteristics of clones change as tumors evolve, with some clone populations expanding in size and others remaining unchanged or becoming extinct. In advanced stages of tumor evolution, tumors might become dominated by single clones.

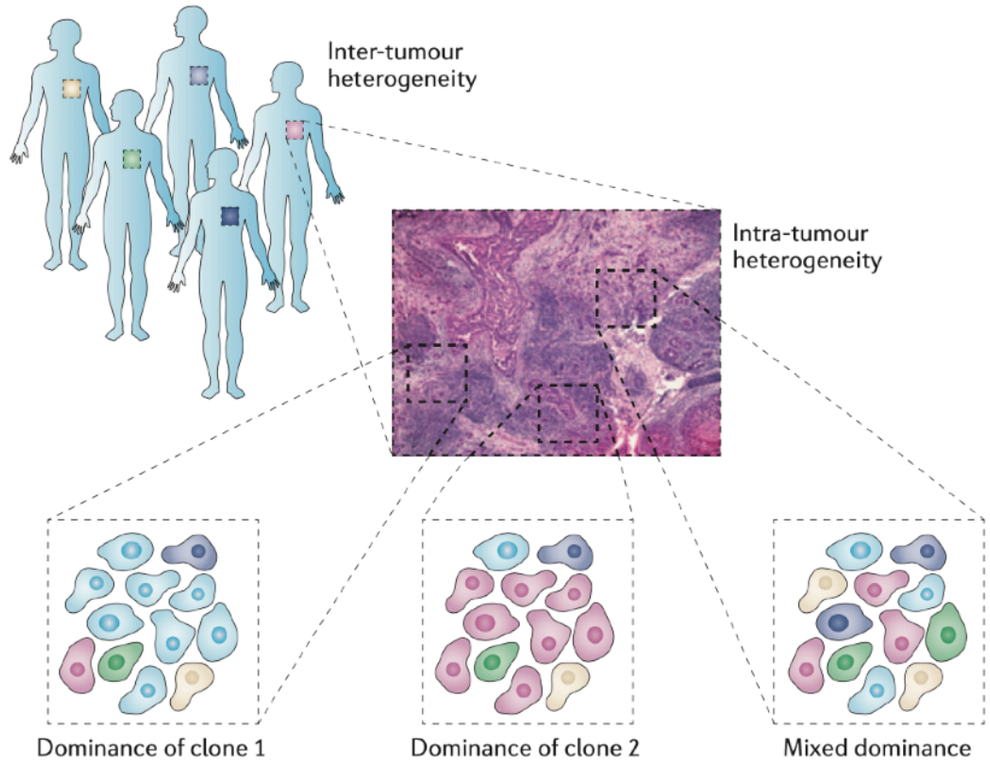

Figure 4 | **Tumour heterogeneity in diagnostics.** Similar to inter-tumour heterogeneity, intra-tumour heterogeneity of cellular phenotypes that result from genetic and non-genetic influences can complicate definitive diagnostics and can obstruct therapeutic decision-making. First, spatial phenotypic heterogeneity can lead to a situation in which a biopsy does not provide an adequate reflection of the phenotypic composition of the whole tumour. Second, decisions made based on scoring the dominant phenotype in a given sample might be misleading if they do not account for minor subpopulations with clinically and biologically important distinct features.

Marusyk & Polyak, Biochimica et Biophysica Acta 2010
Marusyk, Almemdro & Polyak, Nature Reviews Cancer 2012

proliferative signaling/outgrowth are hallmarks of cancer

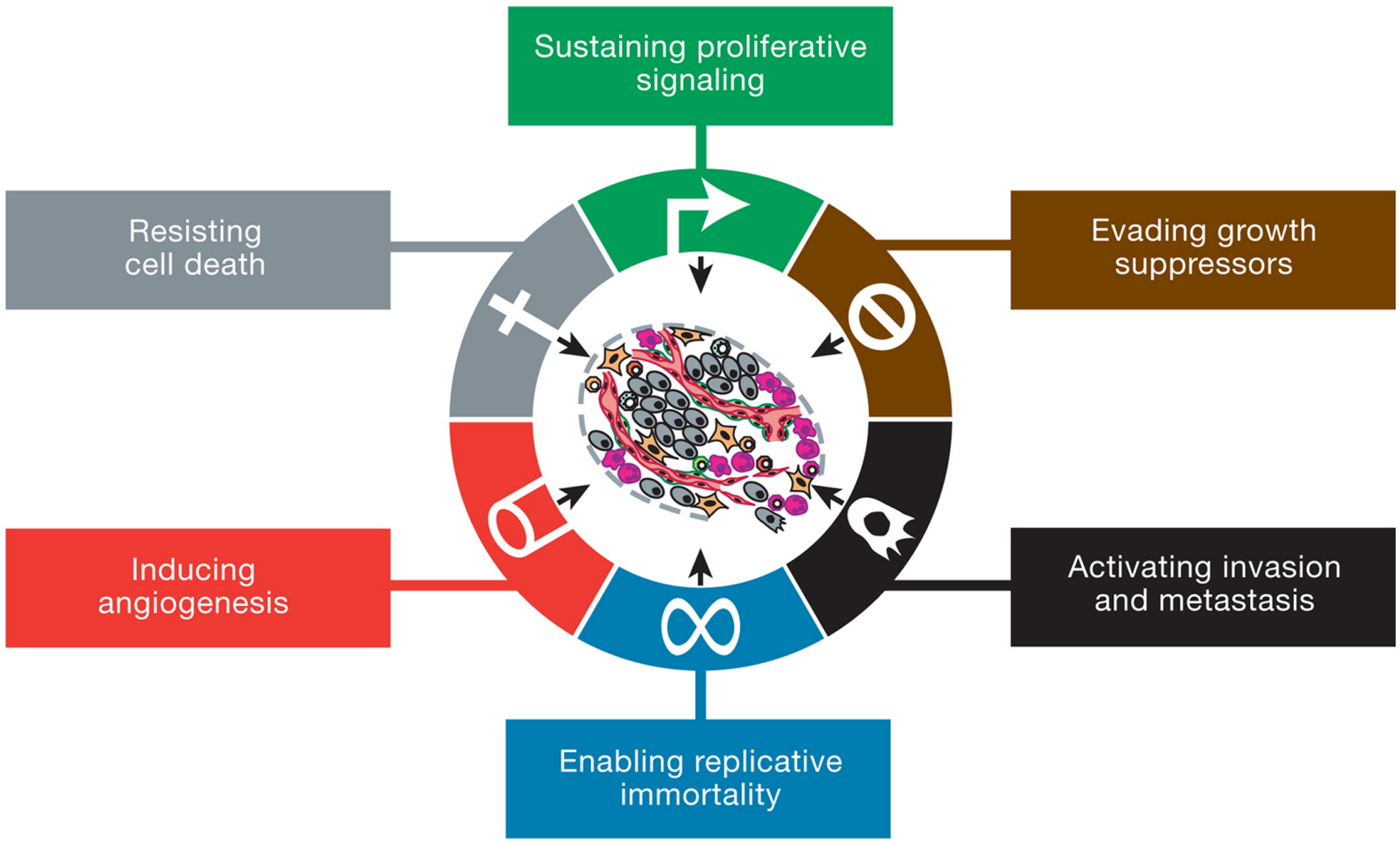

Hanahan & Weinberg, Hallmarks of Cancer: The Next Generation, Cell 2011

Interactions among cancer clones can facilitate heterogeneity (vs. purifying selection)

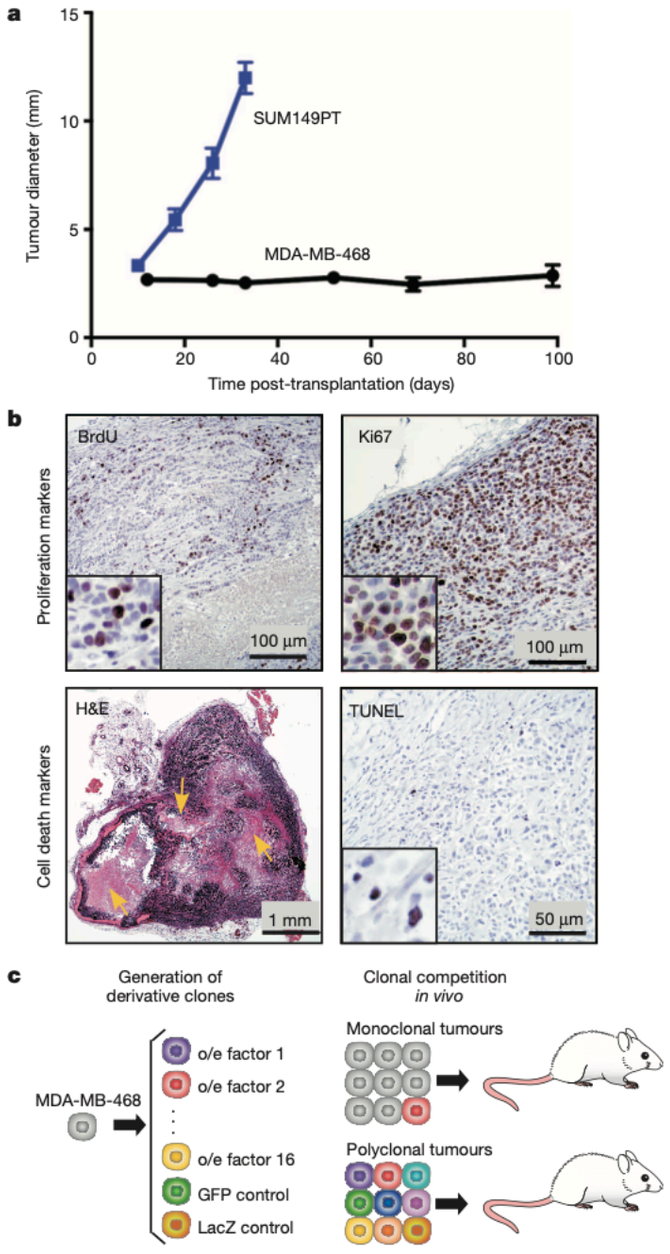

Figure 1 | Experimental system. **a**, Growth of tumours upon mammary fat pad transplantation of indicated cell lines, $n = 10$ per group, combined data from 2 independent experiments, error bars indicate s.e.m. **b**, Representative images of indicated staining. Arrows indicate necrotic areas. H&E, haematoxylin and eosin. **c**, Experimental scheme.

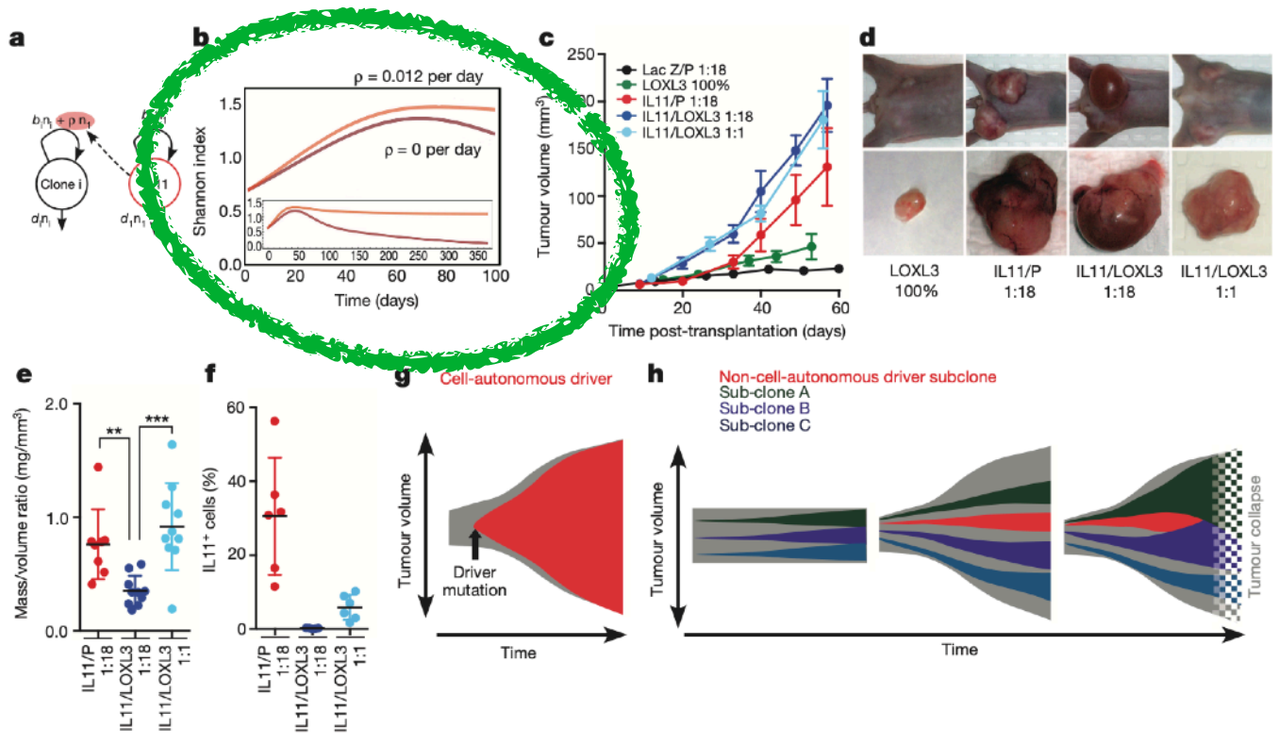

Figure 4 | Effect of IL11 on clonal dynamics. **a**, Outline of the linear model that best explains polyclonal dynamics (see Supplementary Information). **b**, Prediction of diversity over time without (dark) or with (light) non-cell-autonomous driver. **c**, Tumour growth kinetics, $n = 10$ per group. **d**, Representative images. **e**, Mass/volume ratios of tumours in **c**–**e** excluding cyst fluid, each dot represents an individual tumour, $^{**}P < 0.01$, $^{***}P < 0.001$; error bars indicate s.e.m. **f**, Final population frequencies of $IL11^{+}$ cells in the indicated tumours. **g**, **h**, Models of cell-autonomous (**g**) and non-cell-autonomous (**h**) driving of tumour growth. Data shown are representative of at least 2 independent experiments.

non-cell-autonomous driving of tumor growth, together with clonal interference, stabilizes sub-clonal heterogeneity, thereby enabling inter-clonal interactions that can lead to new tumor-phenotypic traits

Marusyk *et al.*, Non-cell-autonomous driving of tumour growth supports sub-clonal heterogeneity, Nature 2014

kinds of interactions in the tumor eco system

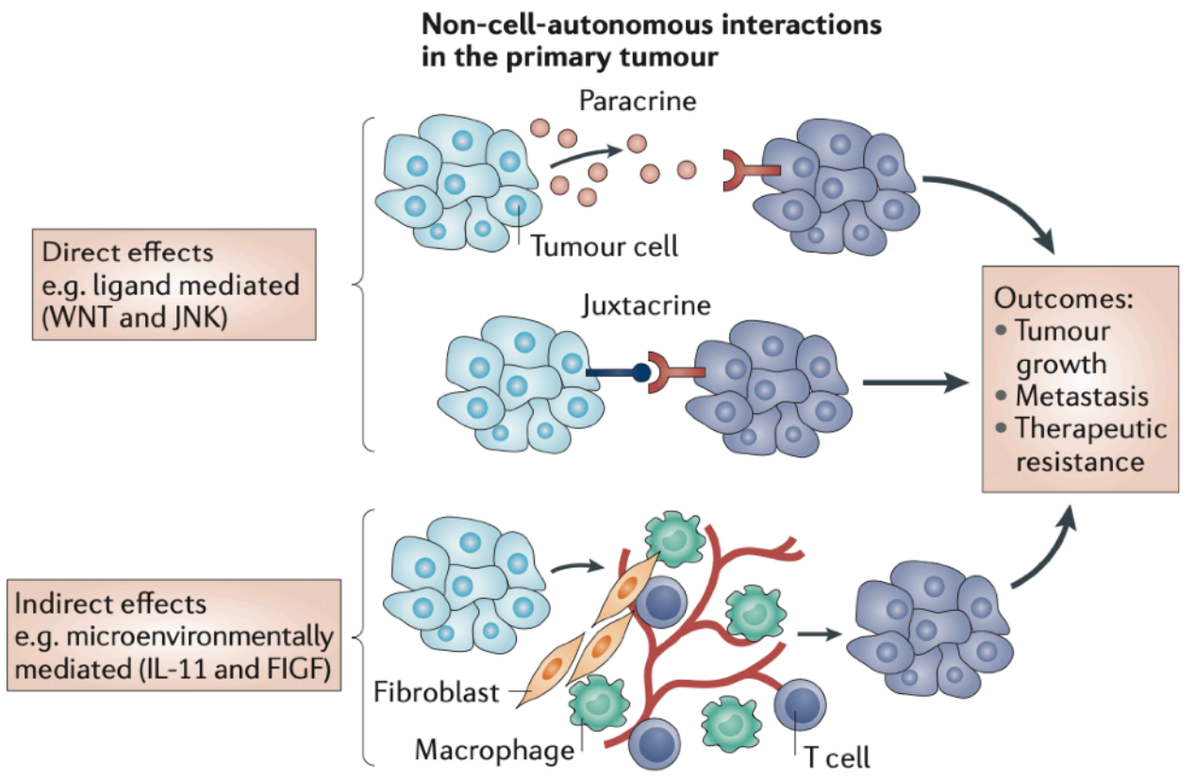

Figure 1 | **Non-cell-autonomous interactions between populations can affect tumorigenesis, metastasis and therapeutic resistance.** Non-cell-autonomous interactions may contribute to increasing the robustness of the tumour, leading to increased tumour growth, enhanced metastasis and the emergence of resistance. As exemplified by two distinct cellular populations communicating in a unidirectional manner, such interactions may occur directly through paracrine[27–29] or juxtacrine effects of ligands[49–52,54] that are produced by one cell and received by the second, or these interactions could also be indirectly mediated via components of the microenvironment, such as blood vessels, immune cells and fibroblasts[28,30,49–51]. FIGF, c-fos induced growth factor; IL-11, interleukin-11; JNK, JUN N-terminal kinase.

Tabassum & Polyak, Nature Reviews Cancer 2015

cells grow, move, some produce, public good diffuses and decays

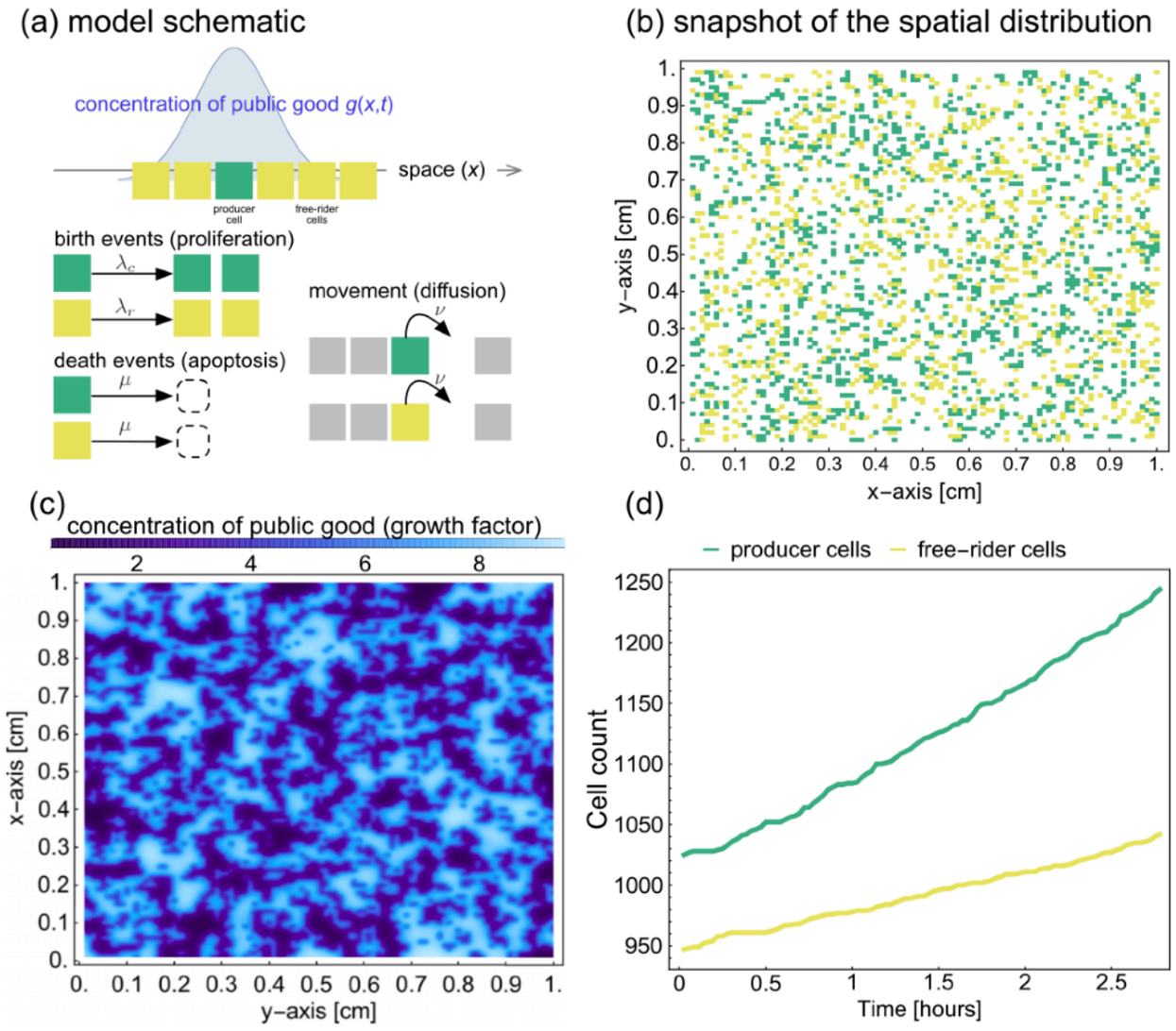

Spectral decomposition of cell densities to derive conditions of the expected growth rate advantage

Exactly describes the dynamics of a randomly assorted population, and serves as good general approximation

Key assumptions: time scale separation, limited dispersal. Gerlee & Altrock, Physical Review E (2019)

growth factors influence competition between producers (C) and non-producers (D)

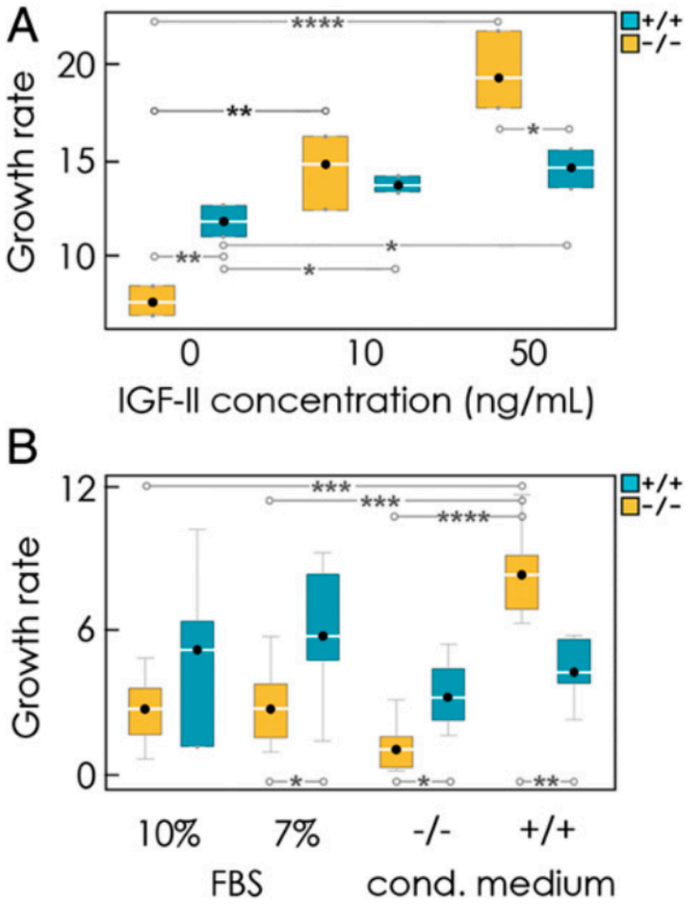

there can be a cost of production

the system can have multiple equilibria

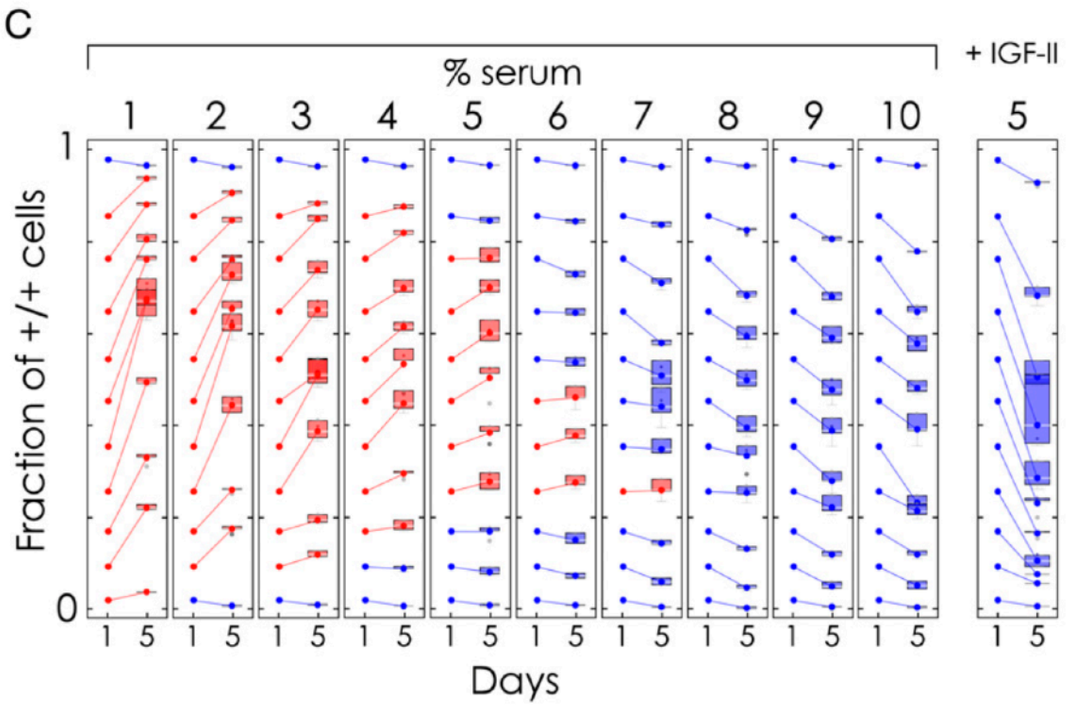

Fig. 1. IGF-II is a nonlinear public good. (*A*) Growth rates of producer (+/+) and nonproducer (–/–) cells in vitro (relative to day 1) at different concentrations of exogenous IGF-II in the growth medium. (*B*) Growth rates of +/+ and –/– cells in vitro (relative to the day with the minimum number of cells) with medium containing FBS (7% or 10%) or in conditioned (cond.) medium from –/– or +/+ cultures. Box plots show the median and the 25% and 75% quartiles (upper and lower fences, respectively). Asterisks show significant *P* values in a *t* test: **P* < 0.05; ***P* < 0.005; ****P* < 0.0005; *****P* < 0.00005.

Archetti *et al*., PNAS 2015. IGF: Insulin-like Growth Factor

nonlinear growth as a function of (locally) available public good

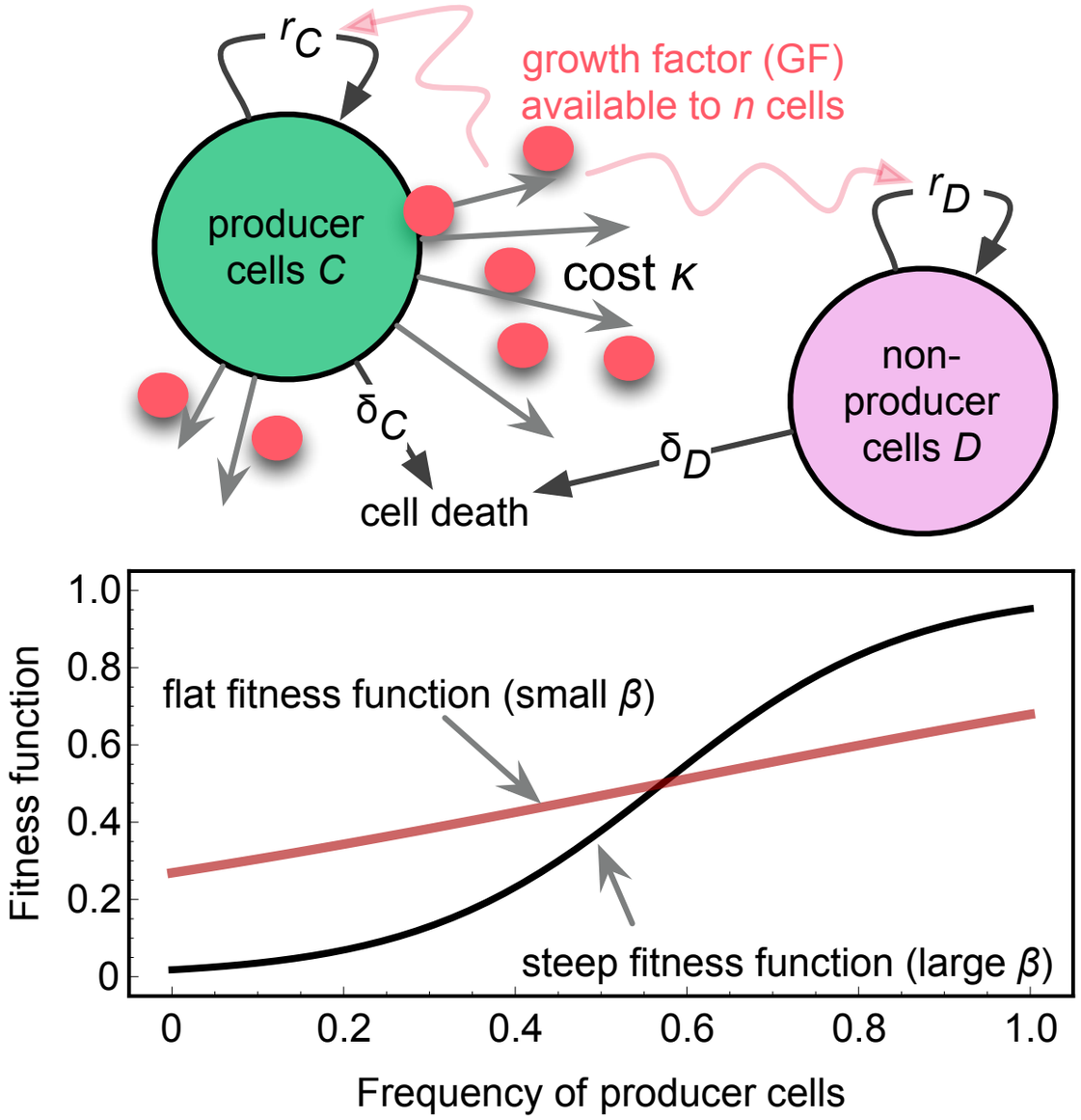

background fitness

$$\lambda(G) = \alpha \frac{1 + e^{\sigma}}{1 + e^{\sigma - \beta G}}$$

good (local)

growth factor concentration

selection coefficient

producer growth: $r_D = \lambda - \kappa$
free-rider growth: $r_D = \lambda$
but the local concentration of *G* might differ

Multiple works by Marco Archetti. Gerlee, Kimmel, Brown & Altrock (2019).
Of note: Hauert, Michor, Nowak, Doebeli. "Synergy and discounting of cooperation in social dilemmas", JTB, 2006.

public good can be shared among a ‘neighborhood’ of size *n*,
a producer cells experience a benefit-to-self

$$r_D = \alpha \frac{1 + \mathrm{e}^{\sigma}}{1 + \mathrm{e}^{\sigma - \beta \frac{n-1}{n} y_C}}$$

$$r_C = \alpha \frac{1 + \mathrm{e}^{\sigma}}{1 + \mathrm{e}^{\sigma - \beta \frac{1 + (n-1) y_C}{n}}} - \kappa$$

population growth (eco-evolutionary dynamics)

$$\dot{x}_C = r_C \left(1 - \frac{x_C + x_D}{K}\right) x_C - \mu_C \, x_C$$

$$\dot{x}_D = r_D \left(1 - \frac{x_C + x_D}{K}\right) x_D - \mu_D \, x_D$$

Kimmel *et al*., Communications Biology, 2019

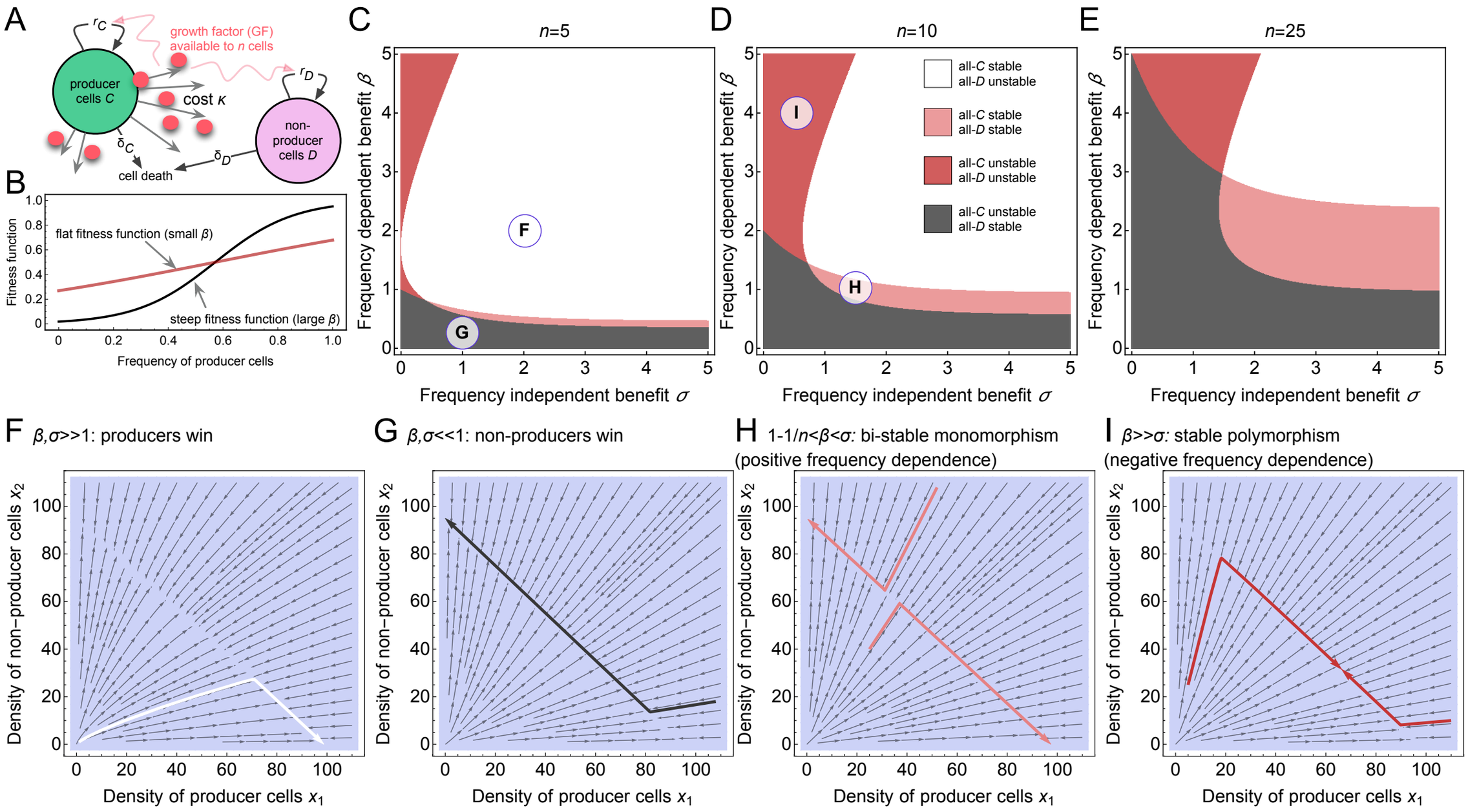
A
producer cells C
non-producer cells D
growth factor (GF) available to n cells
cost κ
cell death
B
flat fitness function (small β)
steep fitness function (large β)
Fitness function
Frequency of producer cells
C
n=5
D
n=10
E
n=25
Frequency dependent benefit β
Frequency independent benefit σ
F
G
H
I
all-C stable all-D unstable
all-C stable all-D stable
all-C unstable all-D unstable
all-C unstable all-D stable
F β,σ>>1: producers win
G β,σ<<1: non-producers win
H 1-1/n<β<σ: bi-stable monomorphism (positive frequency dependence)
I β>>σ: stable polymorphism (negative frequency dependence)
Density of non−producer cells x2
Density of producer cells x1

bifurcations in nonlinear public good

A σ=2, β=5: growth rate difference

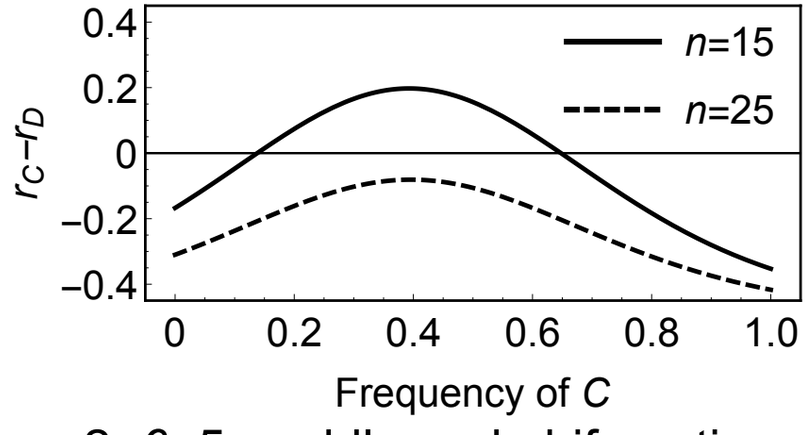

B σ=2, β=5: saddle-node bifurcation

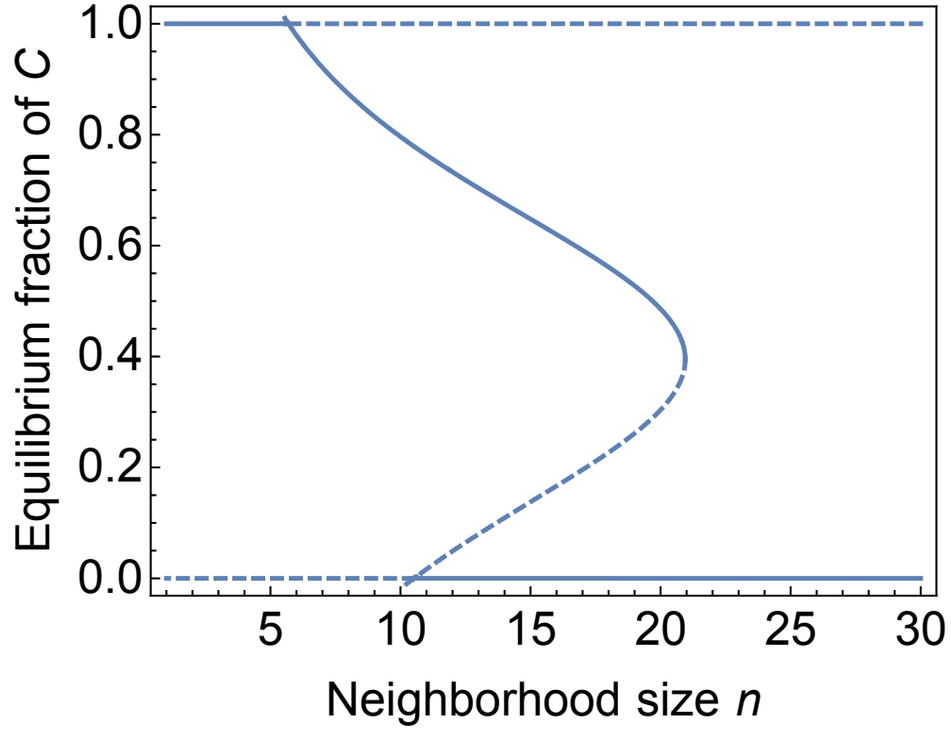

C σ=3, β=2: growth rate difference

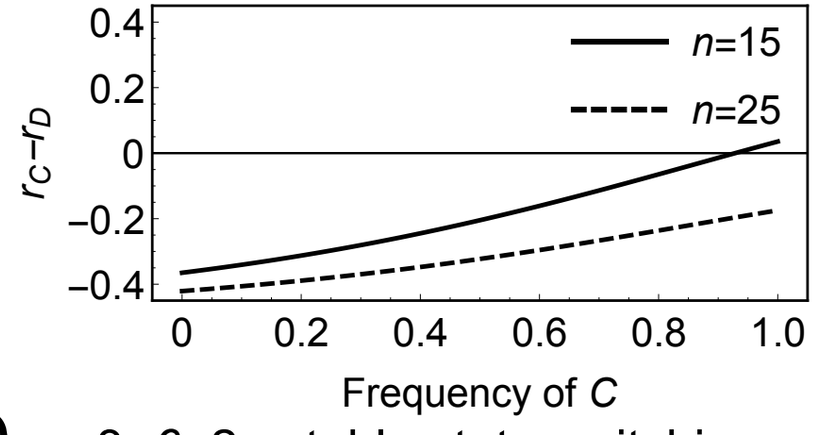

D σ=3, β=2: stable state-switching

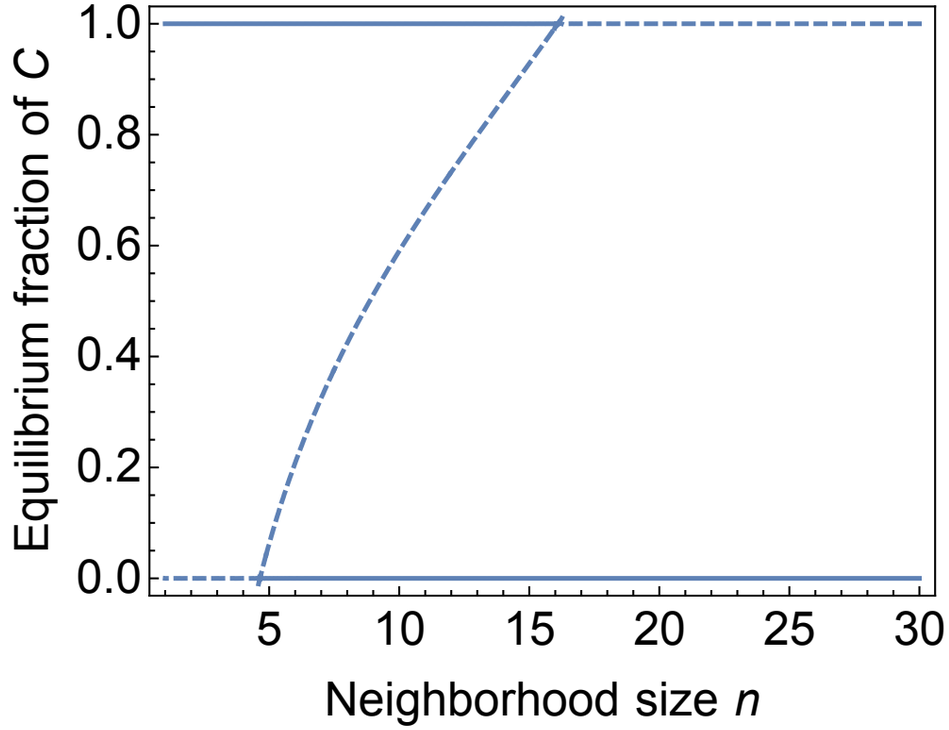

Kimmel *et al*., Communications Biology, 2019

our approach can be used to explain previously measured growth rate differences

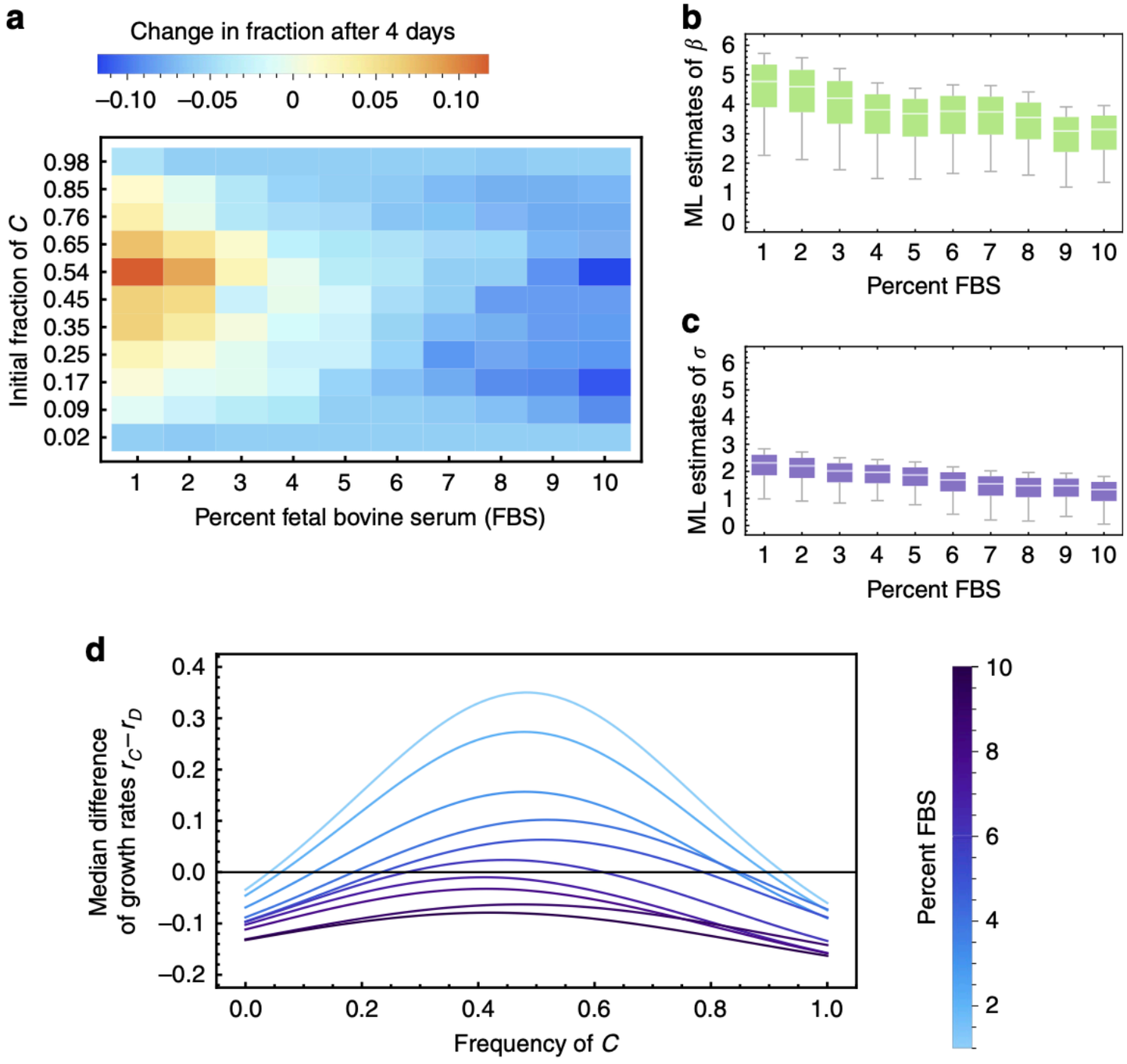

Archetti *et al*., PNAS 2015, Kimmel *et al*., Communications Biology, 2019

stochastic dynamics due to demographic noise

$$C \xrightarrow{\rho_C} C + C$$

$$D \xrightarrow{\rho_D} D + D$$

$$C \xrightarrow{\mu_C} \emptyset$$

$$D \xrightarrow{\mu_D} \emptyset$$

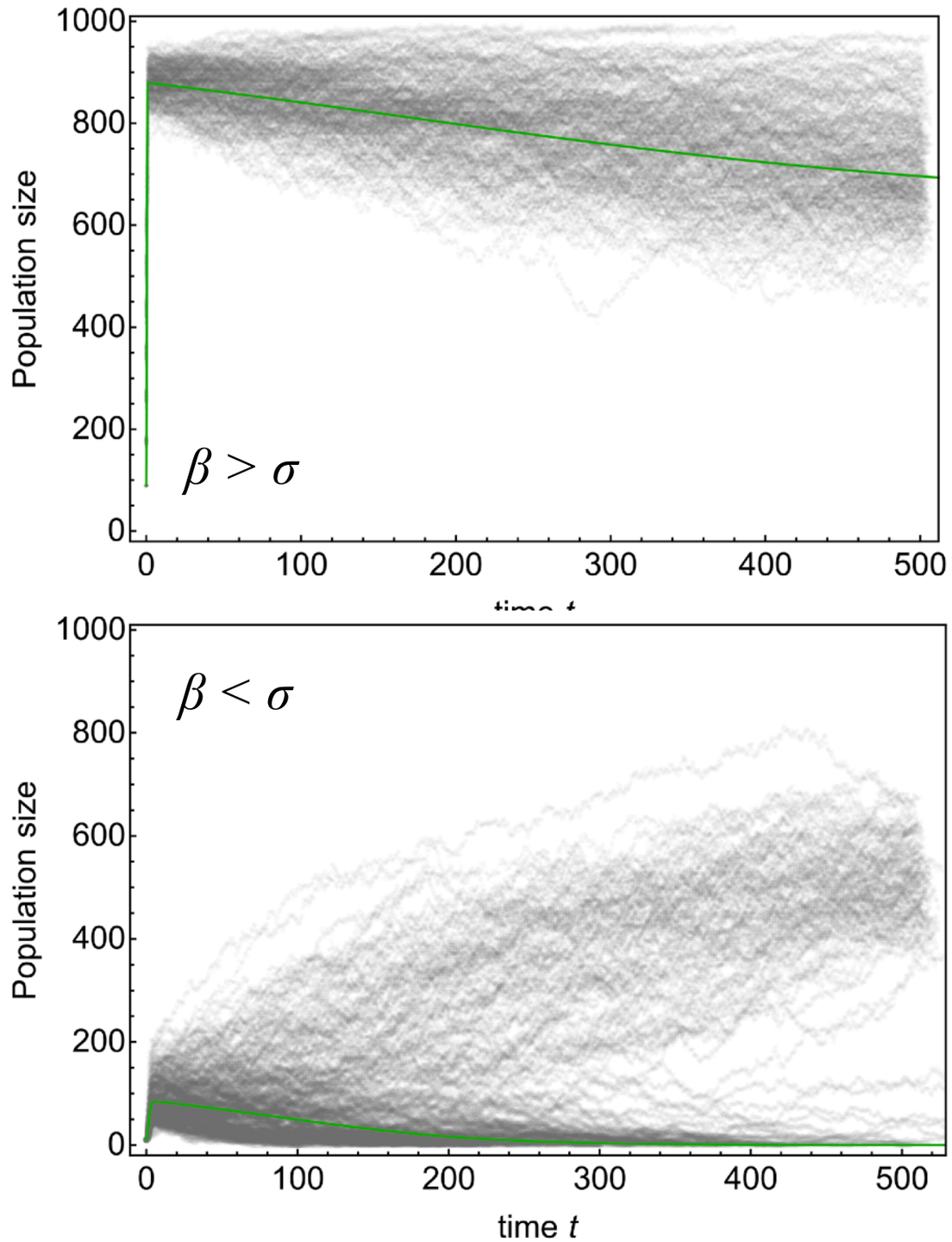

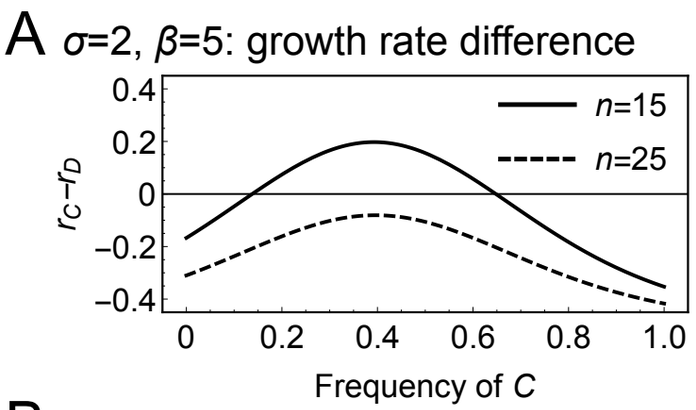
A σ=2, β=5: growth rate difference
0.4
0.2
0
−0.2
−0.4
$r_C - r_D$
n=15
n=25
0
0.2
0.4
0.6
0.8
1.0
Frequency of C

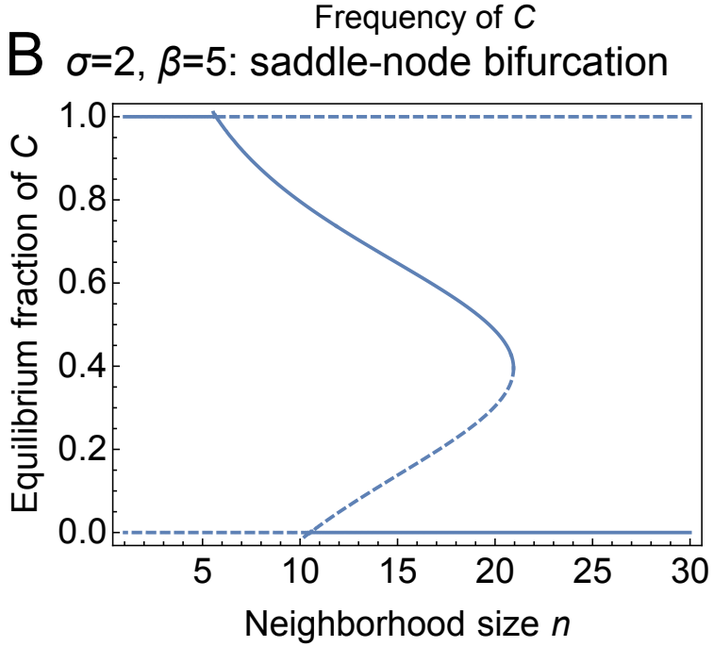
B σ=2, β=5: saddle-node bifurcation
Equilibrium fraction of C
1.0
0.8
0.6
0.4
0.2
0.0
5
10
15
20
25
30
Neighborhood size n

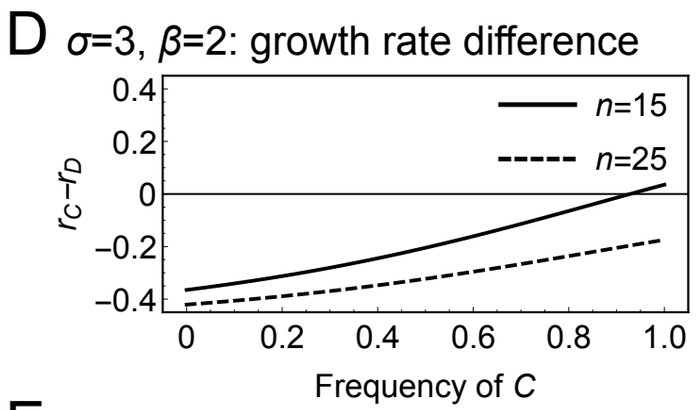
D σ=3, β=2: growth rate difference
0.4
0.2
0
−0.2
−0.4
$r_C - r_D$
n=15
n=25
0
0.2
0.4
0.6
0.8
1.0
Frequency of C

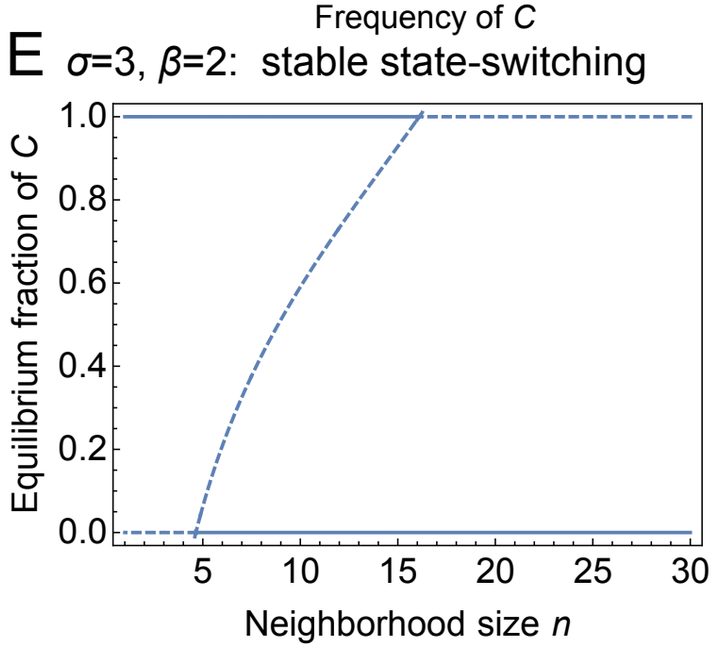
E σ=3, β=2: stable state-switching
Equilibrium fraction of C
1.0
0.8
0.6
0.4
0.2
0.0
5
10
15
20
25
30
Neighborhood size n

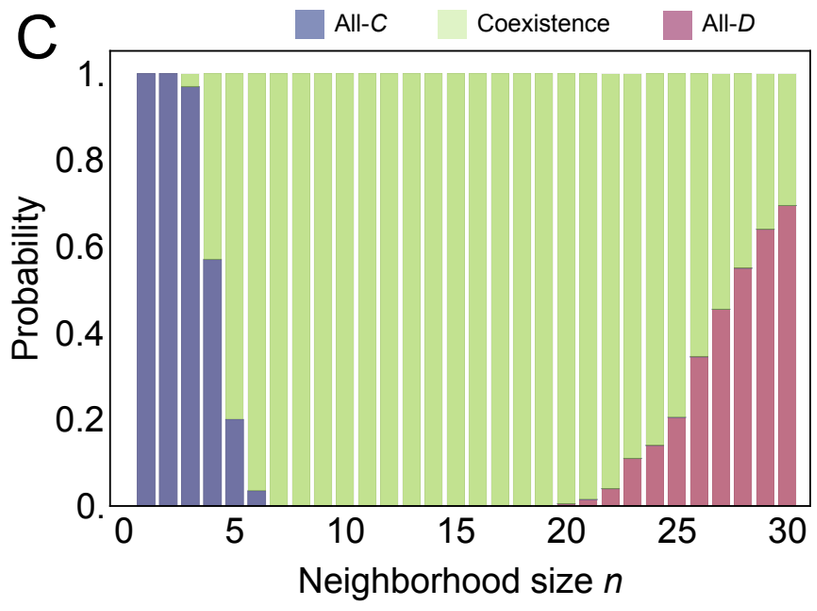
C
All-C
Coexistence
All-D
Probability
1.
0.8
0.6
0.4
0.2
0.
0
5
10
15
20
25
30
Neighborhood size n

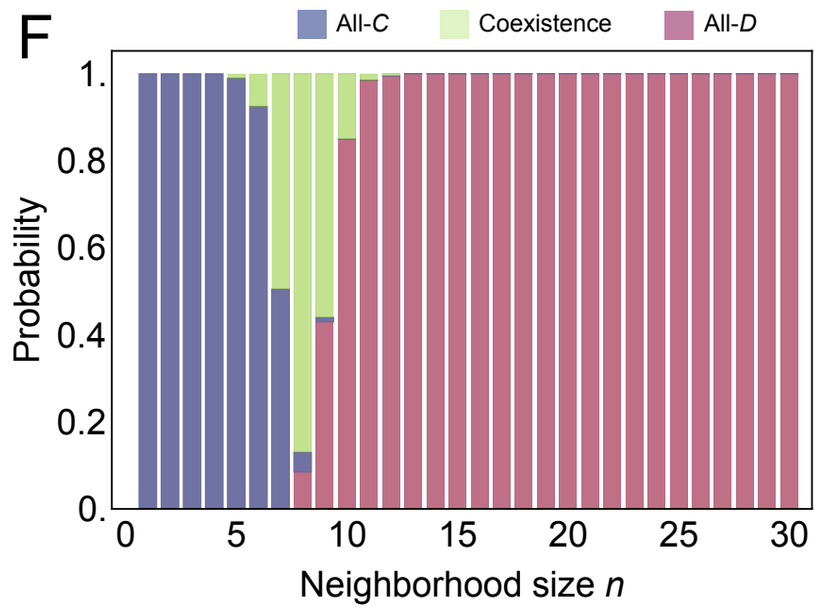
F
All-C
Coexistence
All-D
Probability
1.
0.8
0.6
0.4
0.2
0.
0
5
10
15
20
25
30
Neighborhood size n

the role of population partition: emerging neighborhood size

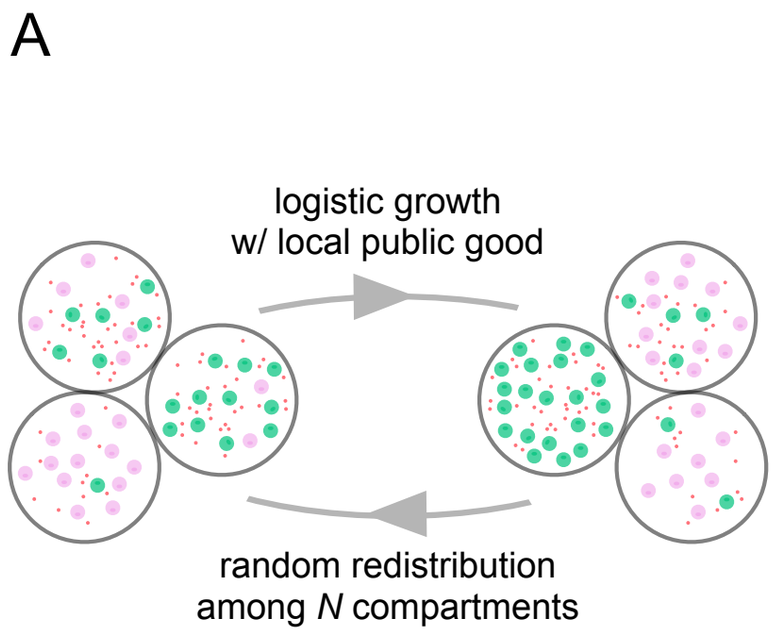

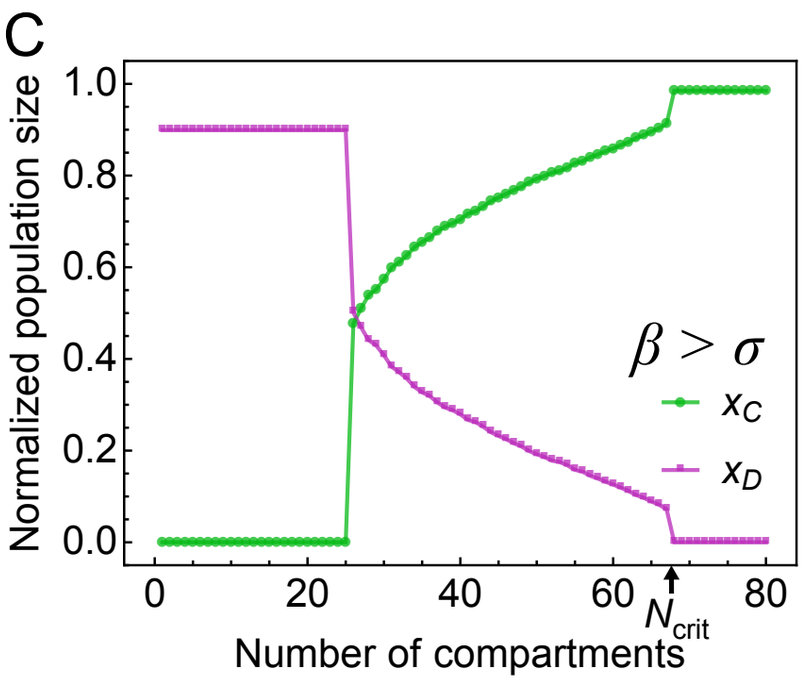

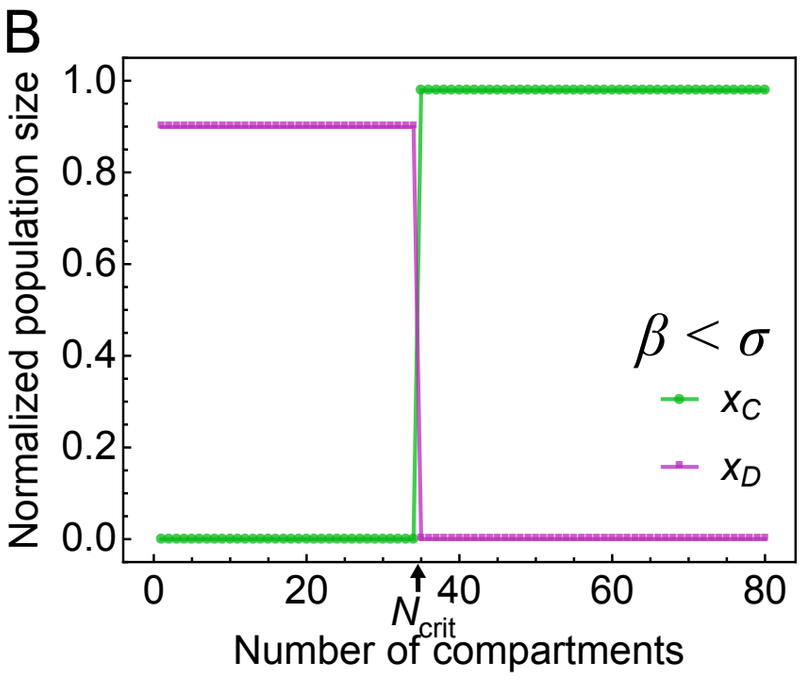

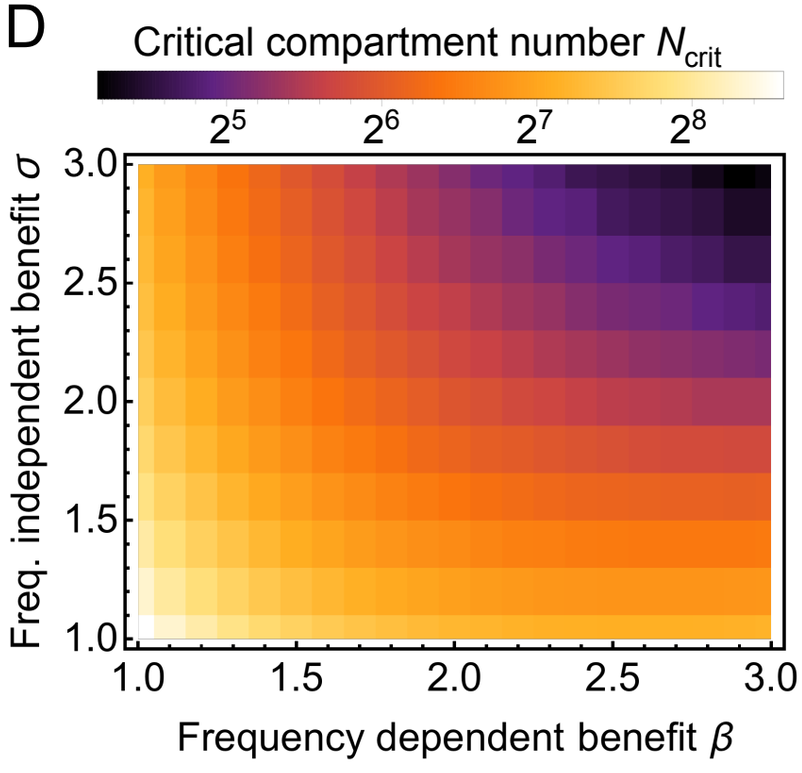

see also works by Cremer, Frey et al. on selection-redistribution models

origins of producers and free-riders in nonlinear public goods games

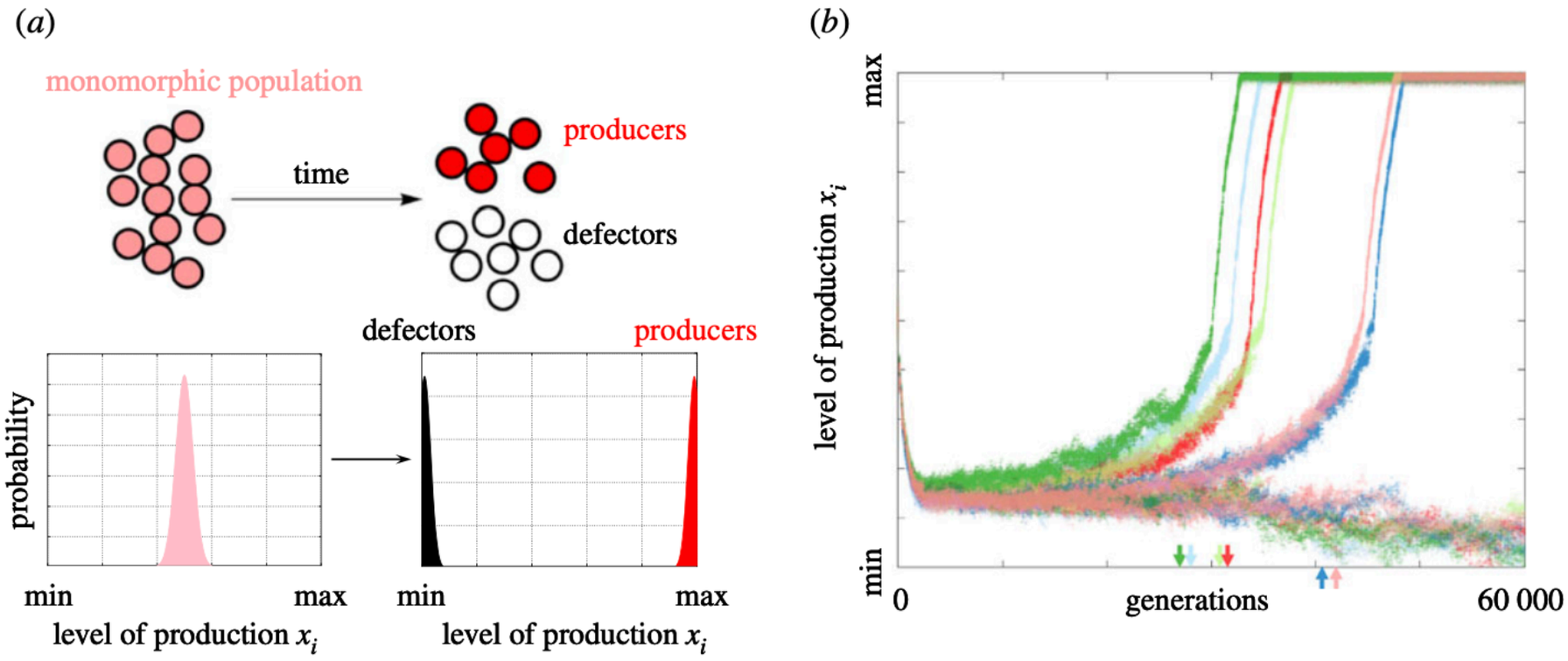

Johnson, Altrock & Kimmel, Royal Society Open Science 2021
Doebeli, Hauert & Killingback, Science 2004

adaptive dynamics in 2D trait space

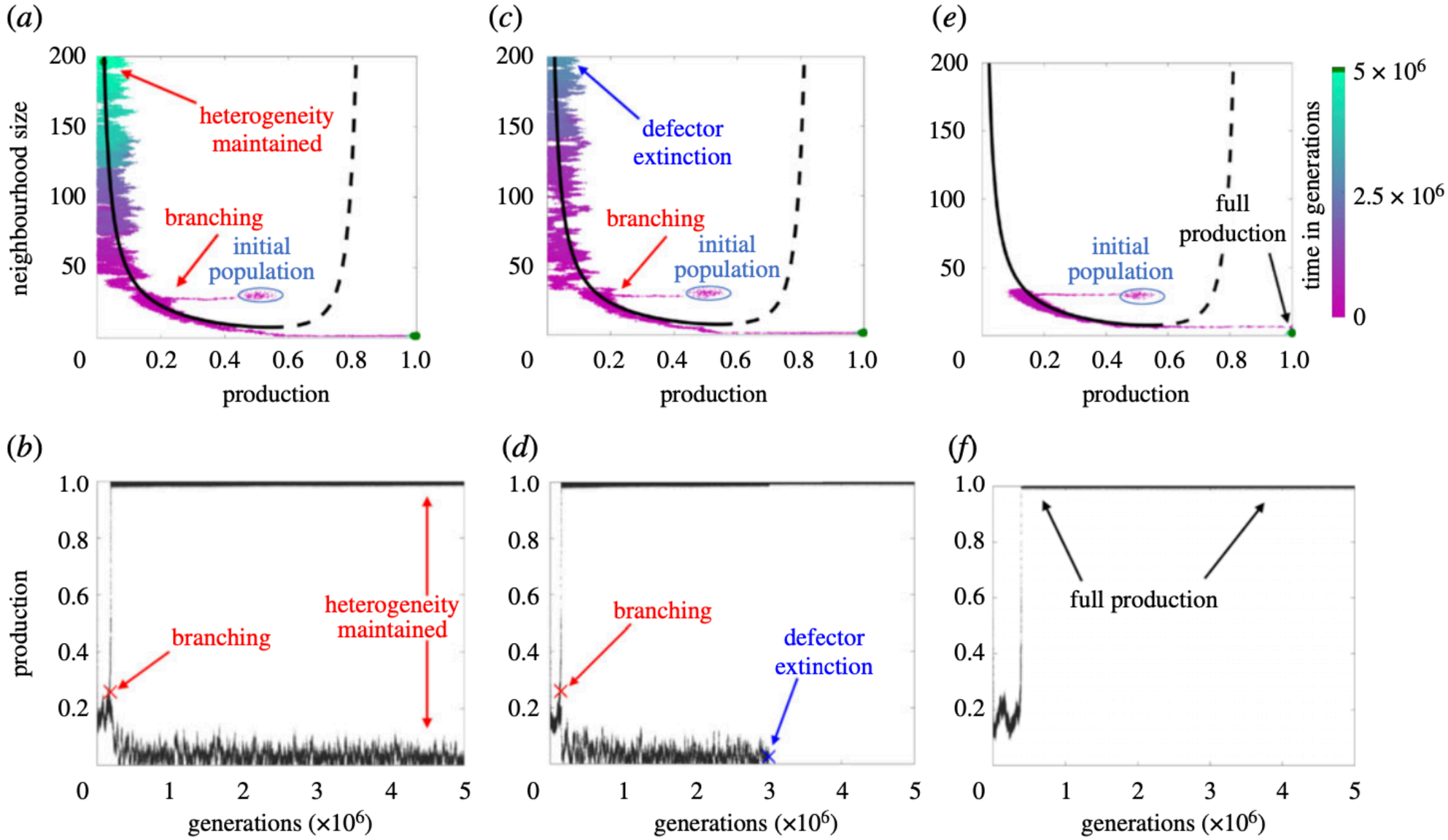

Johnson, Altrock & Kimmel, Royal Society Open Science 2021

evolutionary branching depends on population size

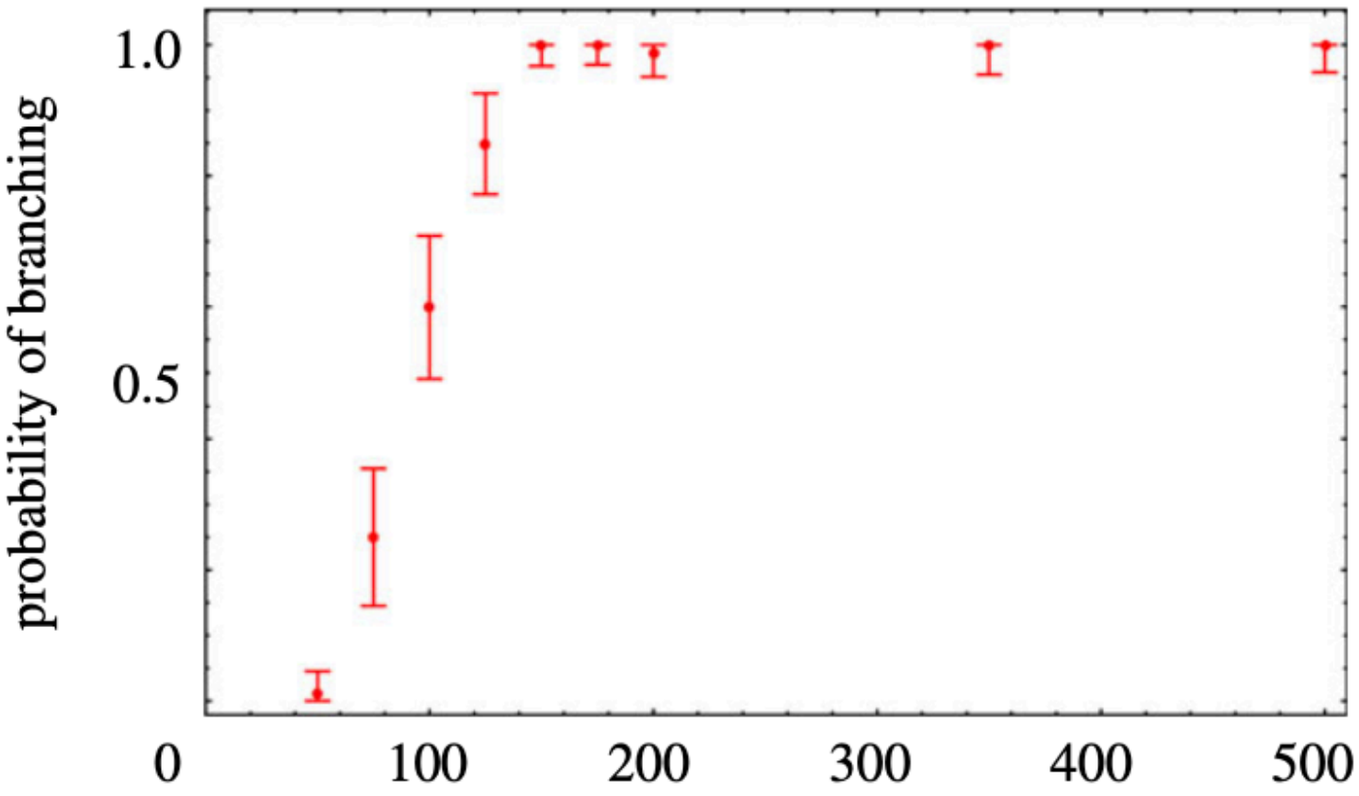

Johnson, Altrock & Kimmel, Royal Society Open Science 2021

summary

Public goods games as a potential mechanism for cancer robustness/progression: non-autonomous expansion (context-dependent selection)

Shared (costly) resources can act as public goods in growing cell populations

Coexistence/producer success is impacted by nonlinearity

Population assortment and demographic noise can lead to producer invasion

Current challenge: how to make these insights more useful for clinical applications?

we want to understand diversity in outcomes based on understanding ecological tumor diversity

a) defining the “neighborhood” of interactions from clinical samples

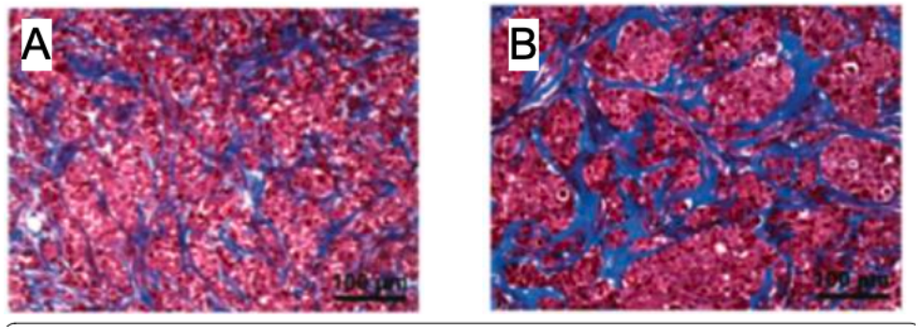

b) protection from growth factors (GFs) during therapy

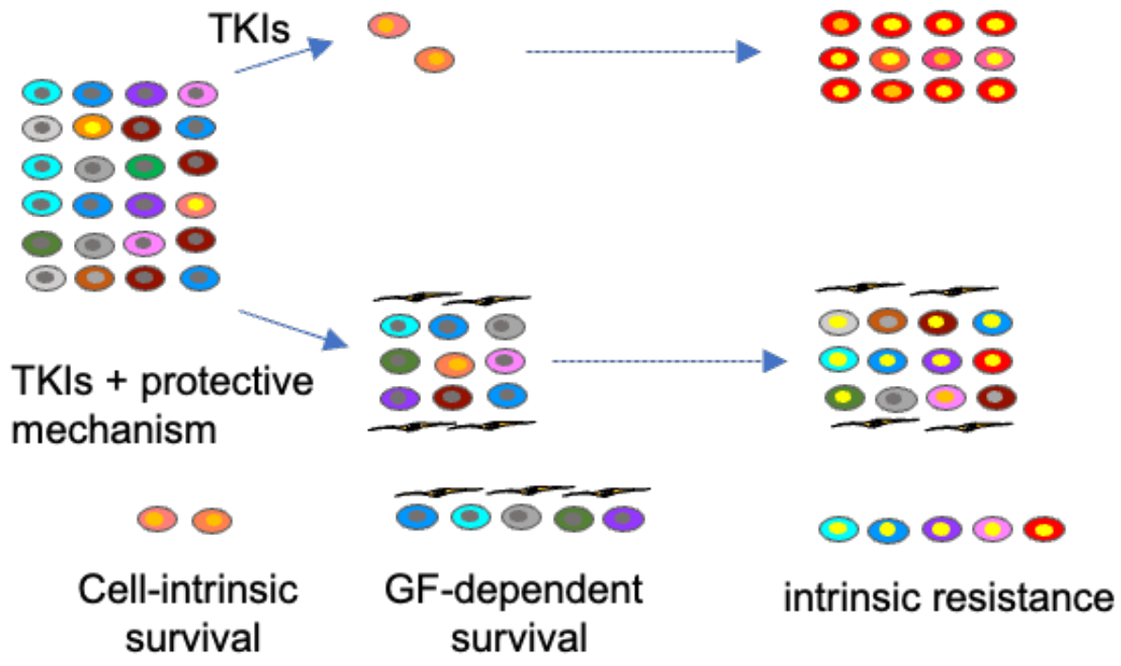

CAF: Cancer Associated Fibroblast. TKI: Tyrosine Kinase Inhibitor

leukemia evolution could be impacted by mutations that evoke public good-like properties

- ‘classical’ drivers: KRAS, NRAS,… may act cell autonomously
- transcription-modifying genes may act non-autonomously
- IDH 1/2 cells can alter self and other cells’ aberrant epigenetic programming (changes methylation, usually increasing), e.g., leading to higher fitness during inflammation

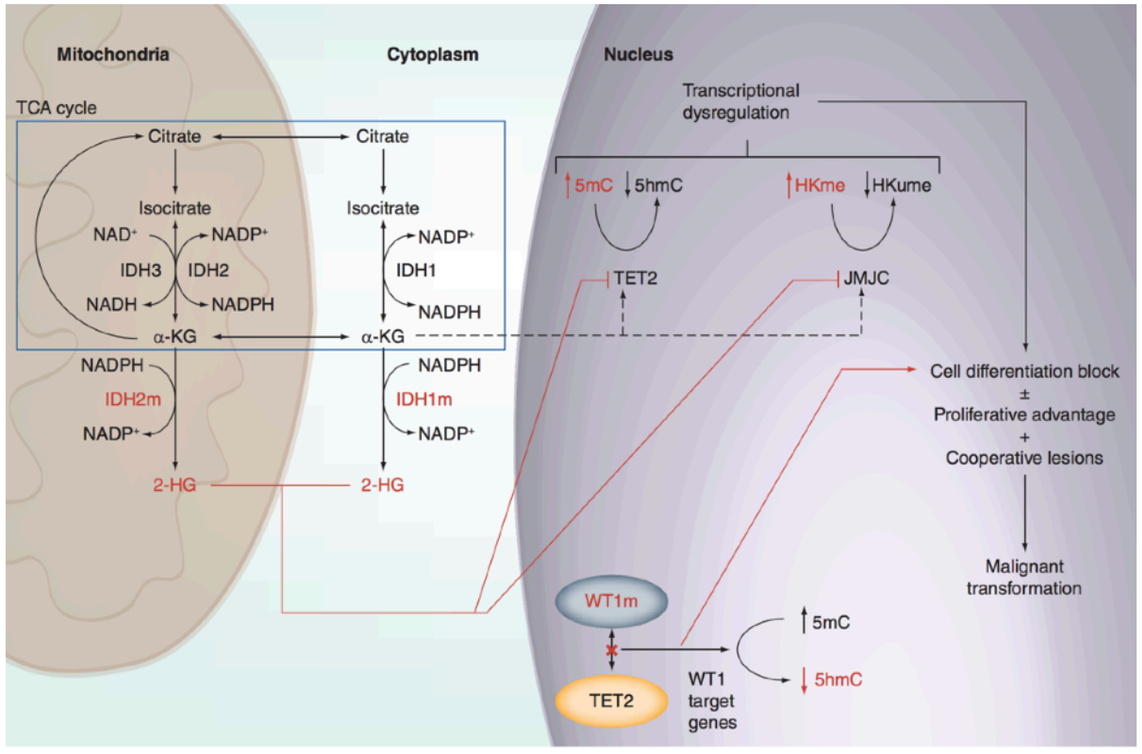

Garrett-Bakelman FE and Melnick AM. Mutant IDH: a targetable driver of leukemic phenotypes linking metabolism, epigenetics and transcriptional regulation. Epigenomics.8:945, 2016.

selection dynamics could inform our understanding of inflammation-driven progression dynamics

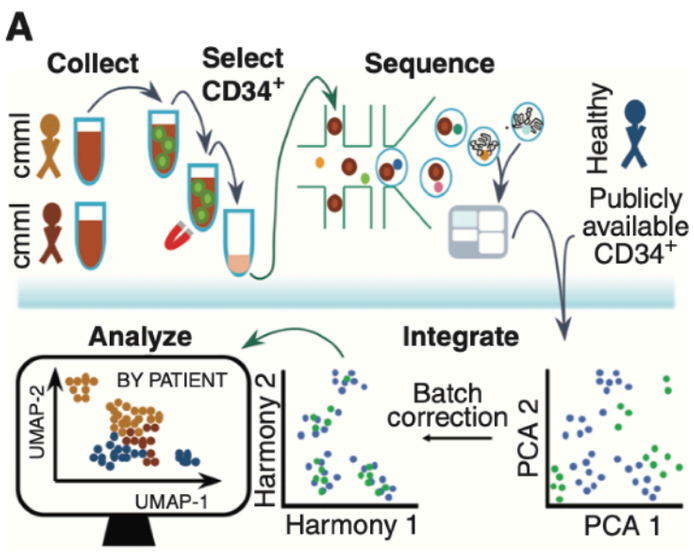

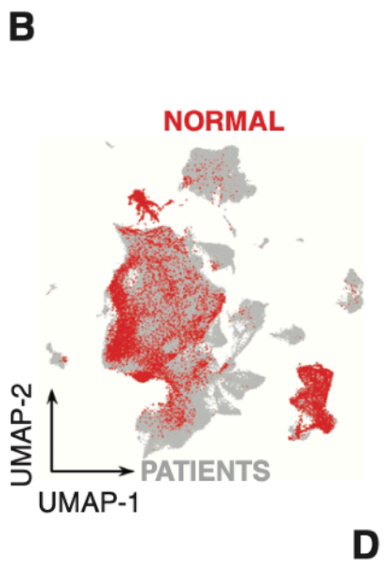

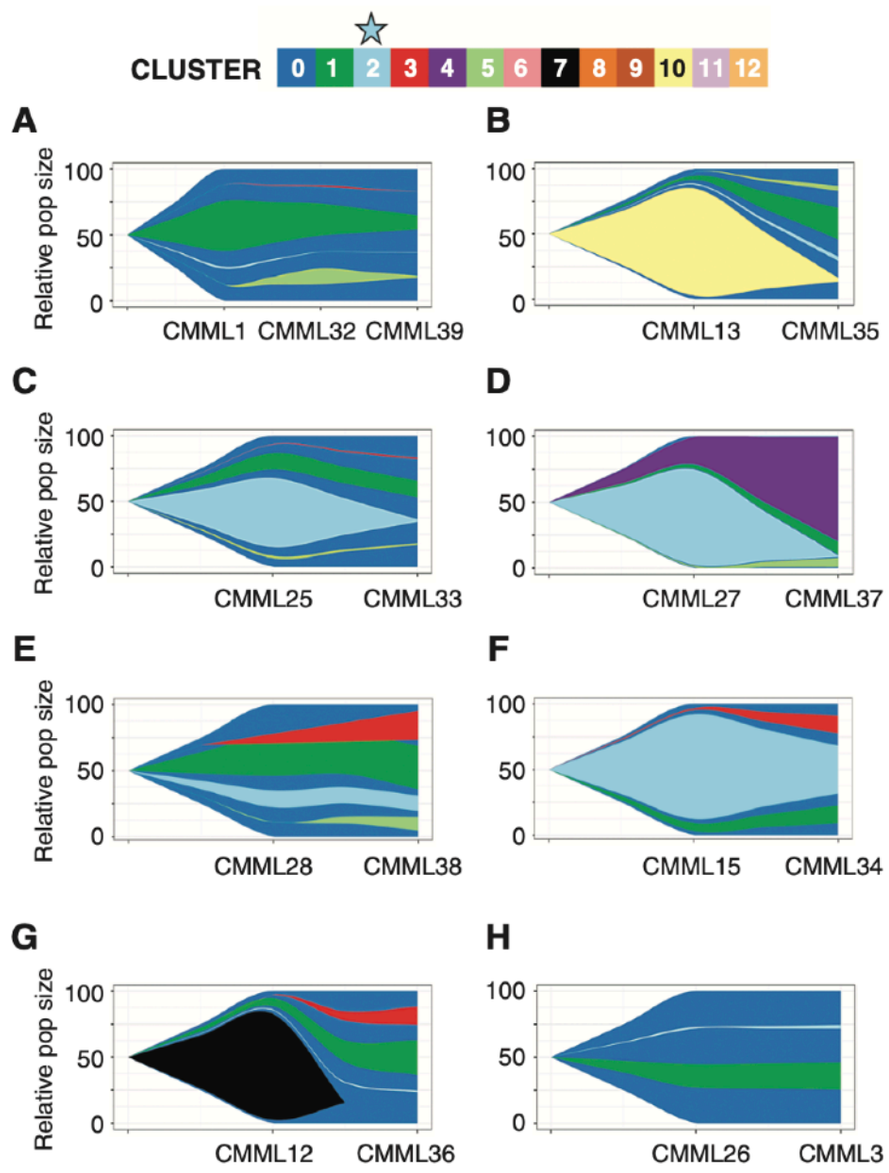

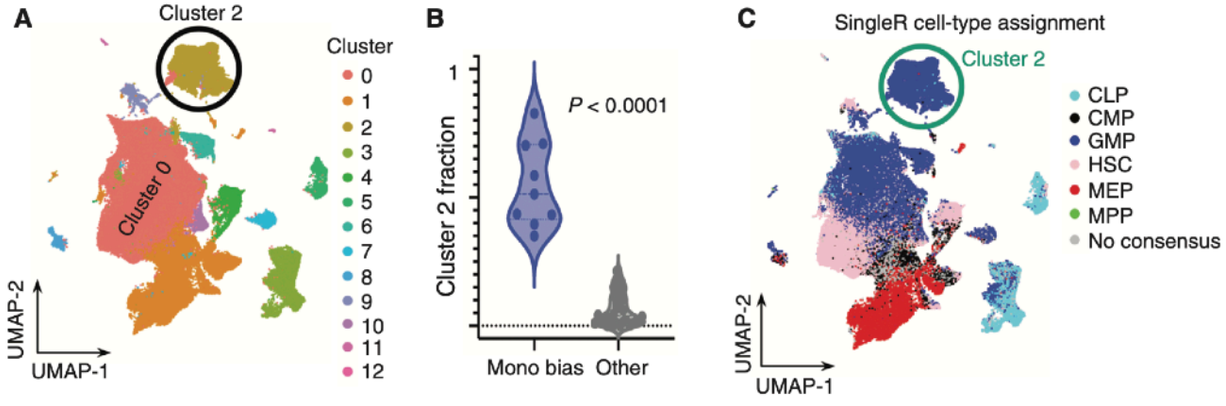

Ferrall-Fairbanks *et al.*, Blood Cancer Discovery (2022).
UMAP: Uniform Manifold Approximation and Projection.
CMML: Chronic Myelomonocytic Leukemia.

Meghan Ferrall-Fairbanks

Brian Johnson

Eric Padron

thanks

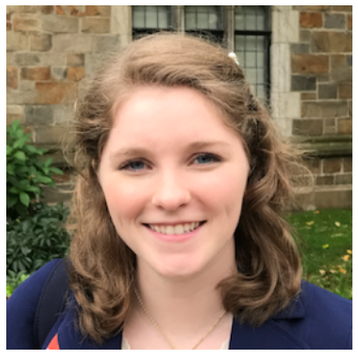

Meghan Ferrall-Fairbanks, PhD
(University of Florida)

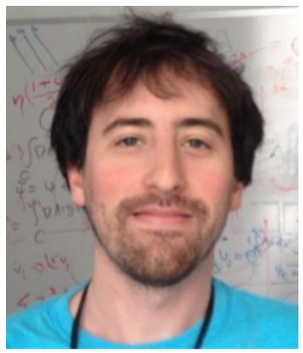

Greg J. Kimmel, PhD
(formerly Moffitt)

Philip Gerlee, PhD
(Chalmers)

Brian Johnson, BSc
(UCSD)

Noemi Andor, PhD
(Moffitt)

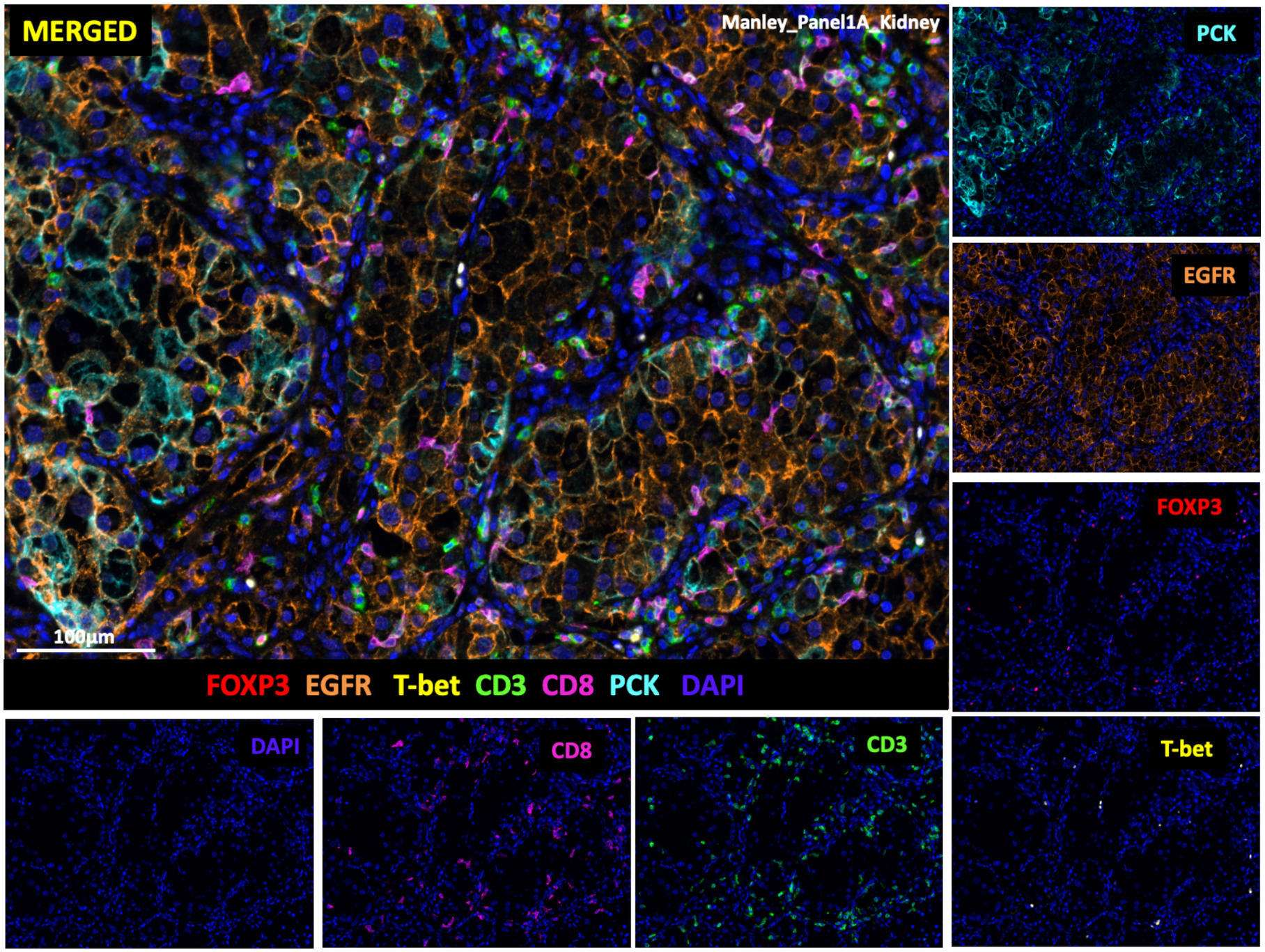

Curtesy of Brandon Manley, MD & Jonathan Nguyen (Moffitt)

public goods in space

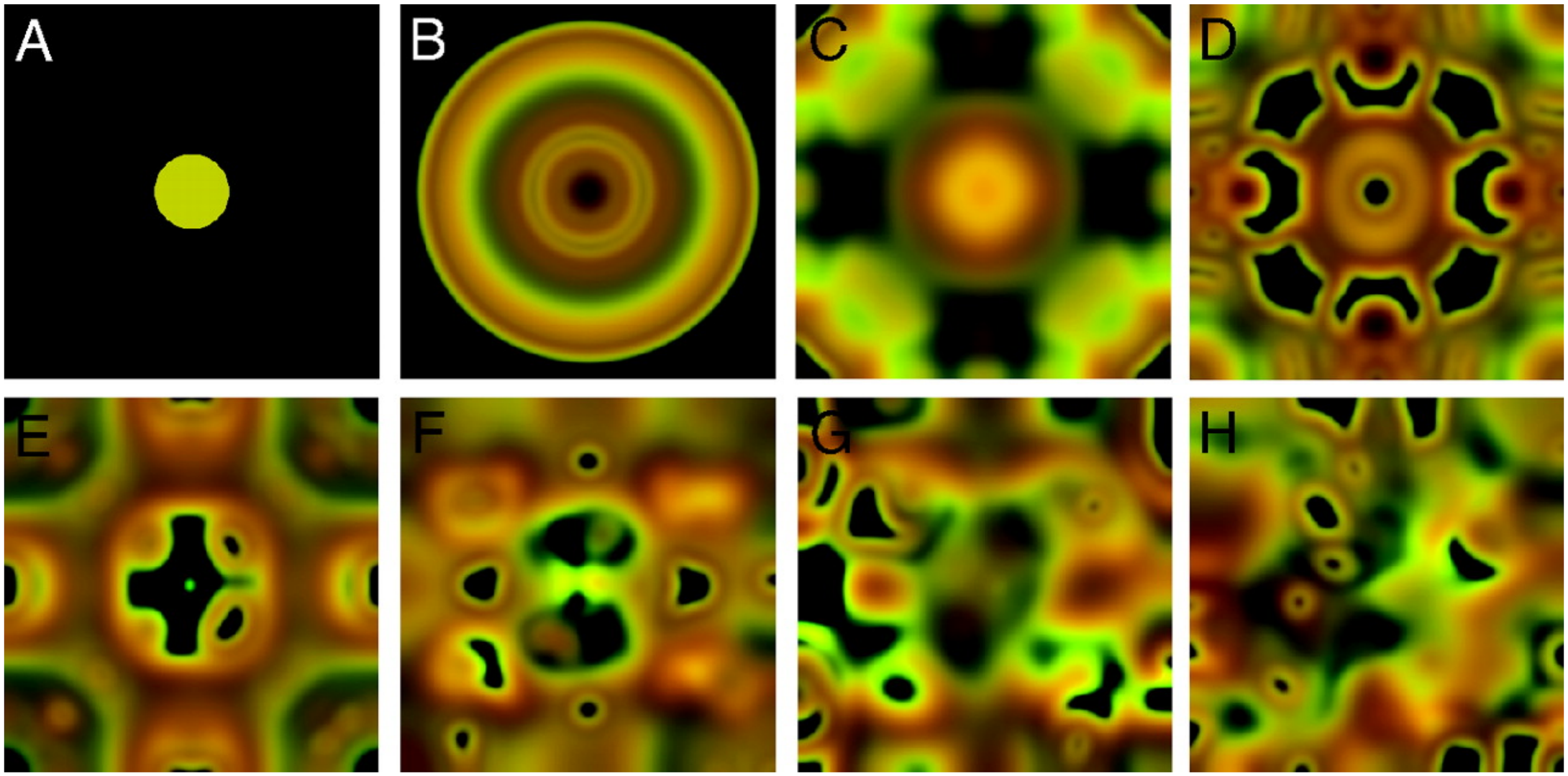

Wakano, Nowak & Hauert, PNAS 2009

coupled equations for producers (U), free-riders (V), and public good (G)

$$\dot{U} = \Gamma_U \nabla^2 U + [\lambda(G) - \kappa][1 - (U + V)]U - \mu_U U,$$

$$\dot{V} = \Gamma_V \nabla^2 V + \lambda(G)[1 - (U + V)]V - \mu_V V,$$

$$\dot{G} = \Gamma_G \nabla^2 G + \rho U - \delta G(U + V).$$

Table 1. Dimensional parameters used in the model given by Eqs (1)–(3). The unit cc^{-1} means per cell cycle.

Parameter	Symbol	Typical ranges (values)	Reference
Producer's diffusion coefficient	Γ_U	$10^{-8} - 10^{-10}$ cm^2/s	[31]
Free-rider's diffusion coefficient	Γ_V	$10^{-8} - 10^{-10}$ cm^2/s	[31]
Public good's diffusion coefficient	Γ_G	$10^{-7} - 10^{-4}$ cm^2/s	[32, 33]
Cellular intrinsic growth rate	α	1 cc^{-1}	
Producer's death rate	μ_U	< 1 cc^{-1}	
Free-rider's death rate	μ_V	< 1 cc^{-1}	
Public good production cost	κ	$\ll 1$ cc^{-1}	[34]
Public good production rate	ρ	100-1000 cc^{-1}	[35]
Public good consumption rate	δ	100-1000 cc^{-1}	
Public good benefit (conc. independent)	σ	1-3	[27]
Public good benefit (conc. dependent)	β	2-6 [conc.]$^{-1}$	[27]
Characteristic length of spatial domain	L	1-10 cm	

https://doi.org/10.1371/journal.pcbi.1007361.t001

rescaling to dimensionless quantities

$$\dot{U} = \gamma_U \nabla^2 U + (\lambda(G) - 1 + a)[1 - (U + V)]U - cU,$$

$$\dot{V} = \gamma_V \nabla^2 V + \lambda(G)[1 - (U + V)]V - crV,$$

$$\epsilon \dot{G} = \nabla^2 G + U - G(U + V).$$

Table 2. Definition of non-dimensional parameters used in the model given by Eqs (5)–(7). Ranges are given as well as the typical values used throughout the text. $\varepsilon_{\text{exit}}$ is used to determine the ε-extinction or fixation events.

Dimensionless parameter	Symbol	Identity	Range	Typical value
Producer's diffusion coefficient	γ_U	$\frac{\Gamma_U \delta}{\Gamma_G \alpha}$	$10^{-4} - 10^{2}$	0.5
Free-rider's diffusion coefficient	γ_V	$\frac{\Gamma_V \delta}{\Gamma_G \alpha}$	$10^{-4} - 10^{2}$	0.5
Producer (PG independent) birth rate	a	$1 - \frac{\kappa}{\alpha}$	0.75-0.9	0.9
Producer death rate	c	$\frac{\mu_U}{\alpha}$	0-1	0.5
Ratio of free-rider to producer death rate	r	$\frac{\mu_V}{\mu_U}$	> 0	1.0
Ratio of cell birth rate to consumption rate	ϵ	$\frac{\alpha}{\delta}$	$10^{-3} - 10^{-2}$	2×10^{-3}
Neighborhood of a fixed point		$\varepsilon_{\text{exit}}$		10^{-8}

https://doi.org/10.1371/journal.pcbi.1007361.t002

dynamics in highly structured initial populations (domain of free-riders taking over producers)

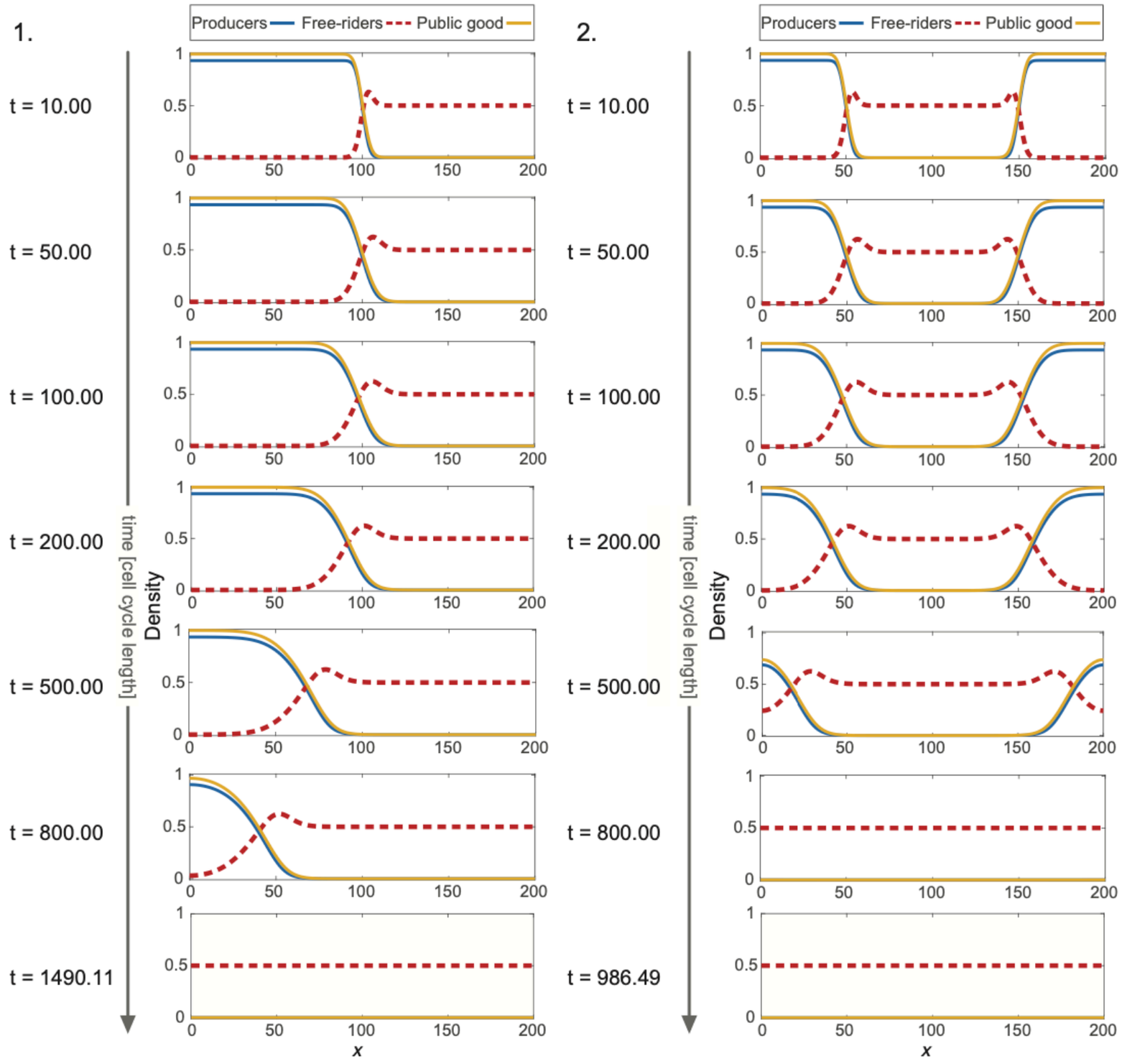

the system is dominated by a slow manifold, for which we can neglect space

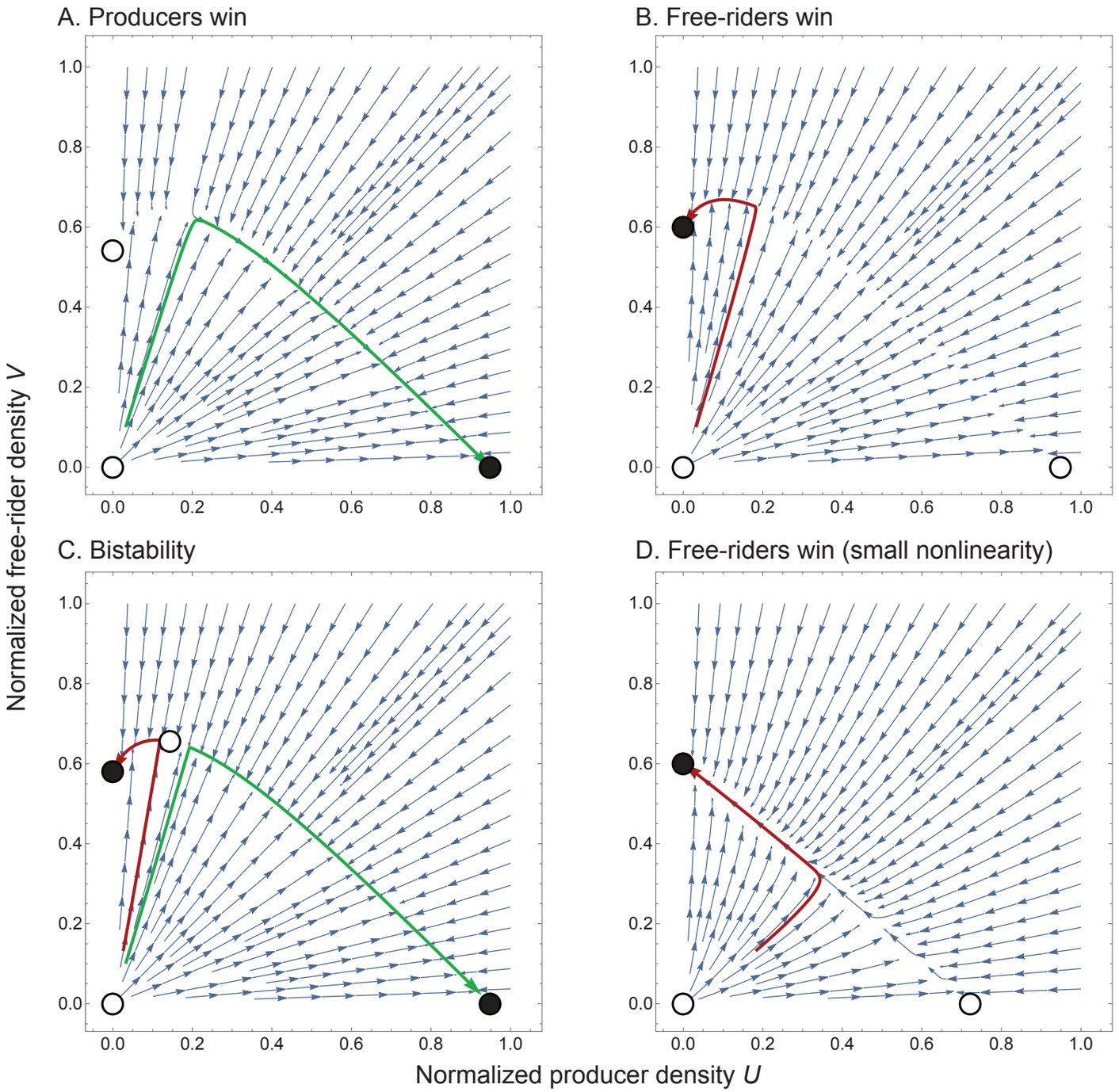

the system is dominated by a slow manifold and extinction times can be calculated

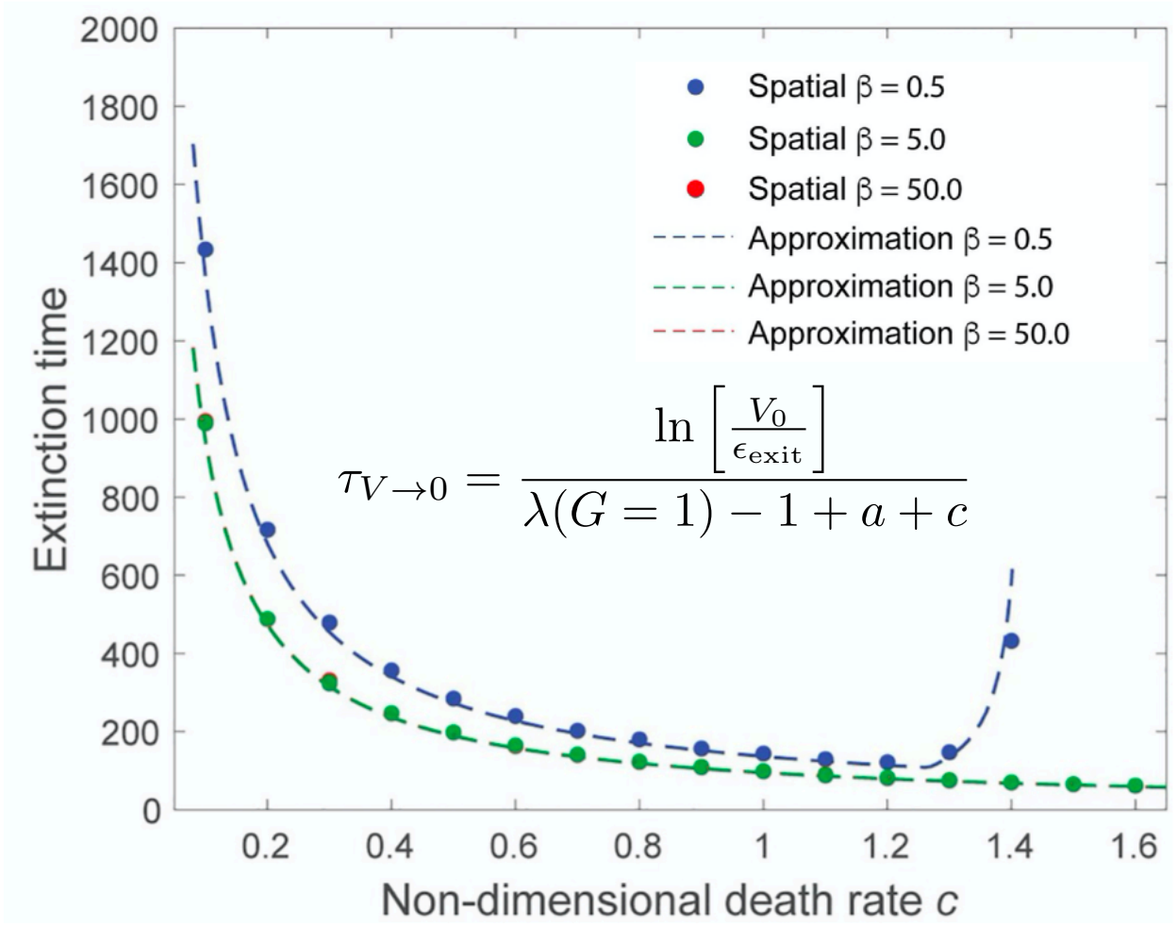

$$\tau_{V\to 0} = \frac{\ln\left[\frac{V_0}{\epsilon_{\text{exit}}}\right]}{\lambda(G=1) - 1 + a + c}$$

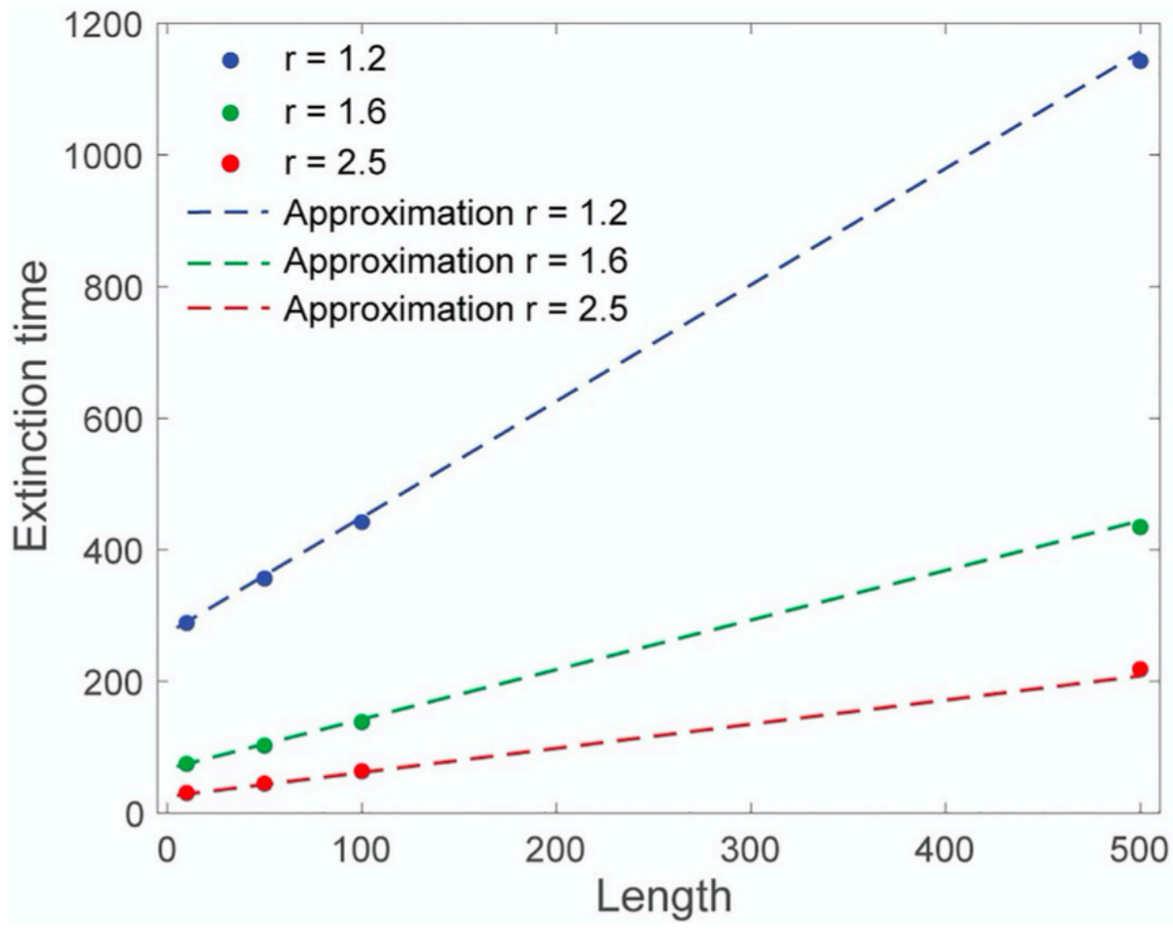

Analytical approximation of ε-extinction time for producer cells to take over.
r = ratio of death rates. *c* = death to birth ratio.
For weak nonlinearity *β*, another singularity emerges at higher *c.*

Kimmel, Gerlee & Altrock, PLoS Computational Biology, 2019

what can we say for highly structured initial conditions?

$$\dot{u} = D\nabla u + r\,u(1-u)$$

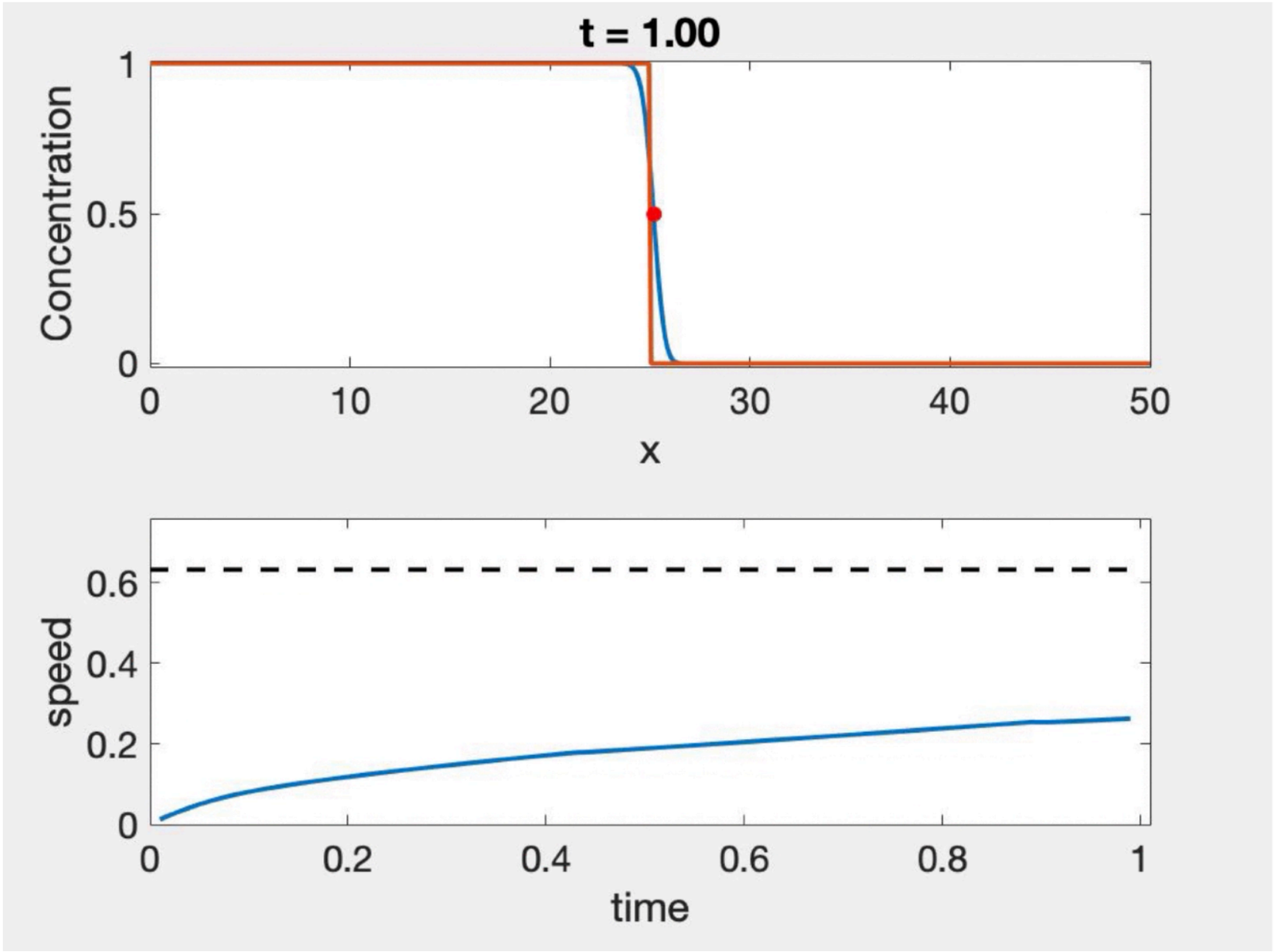

estimating the speed leveraging that only propagation times change

$$t_{\text{total}} = t_{\text{formation}} + t_{\text{propagation}}(d) + t_{\text{boundary}}$$

$$\text{speed} \propto \frac{d_2 - d_1}{t_2 - t_1}$$

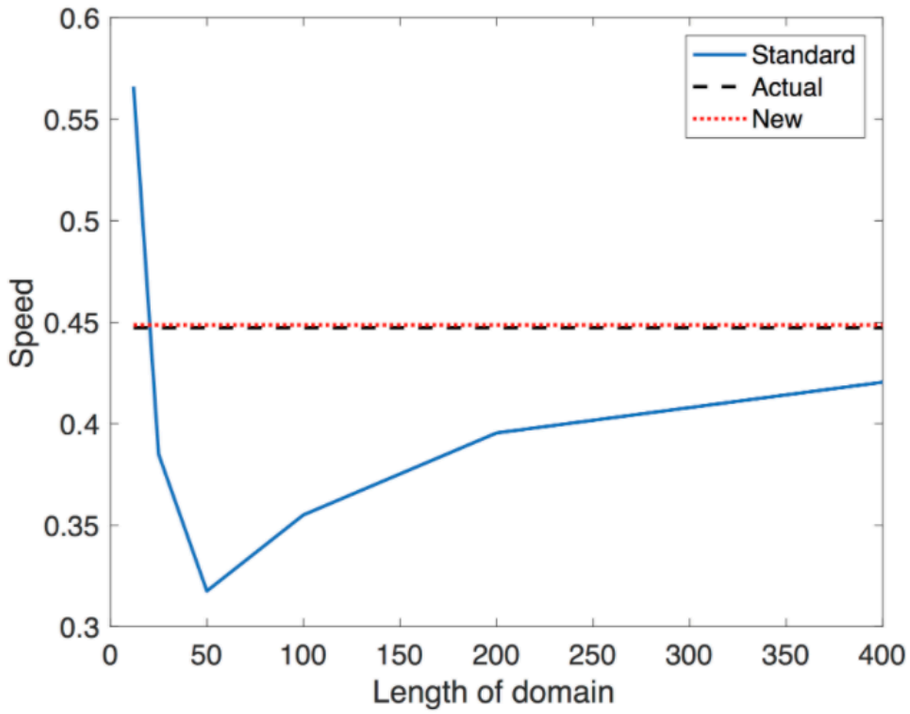

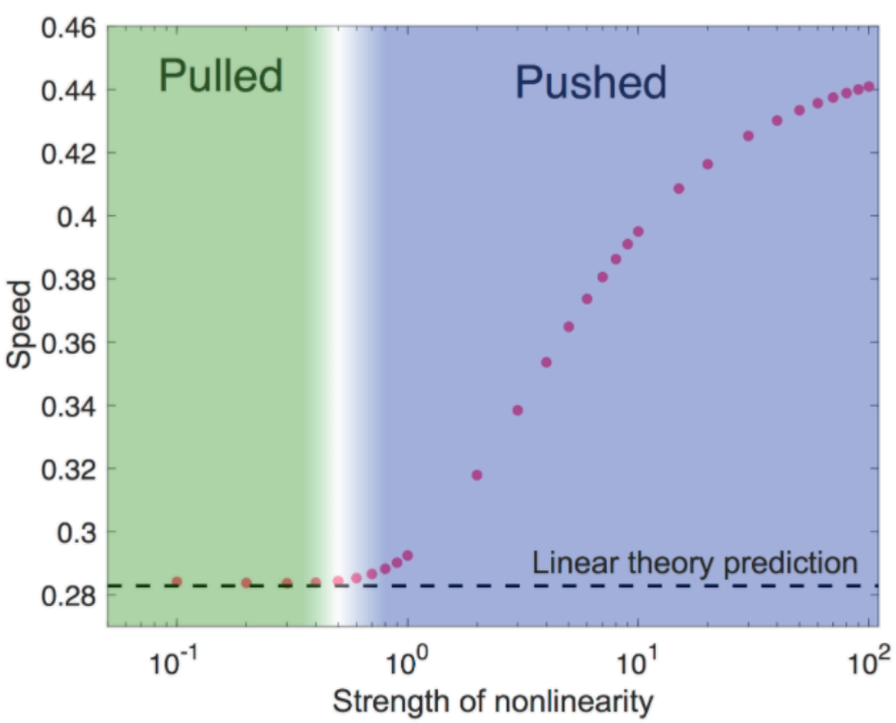

The degree of nonlinearity in the public good drives wave speeds that can be predicted using a simple numerical approach, using same IC (say a wall at L/2) but two domain lengths.

Kimmel, Gerlee & Altrock, PLoS Computational Biology, 2019. See also: Birzu, Hallatschek & Korolev, PNAS, 2018

Stability of the non-spatial system

- Extinction state: $(0, 0, G^0)$ where $G^0 \in [0, 1]$. This state is stable if $\lambda(G^0) < \min(cr, 1 - a + c)$.
- Producers win: $\left(1 - \frac{c}{\lambda(1)-1+a}, 0, 1\right)$. This state is stable if $a > 1 - \lambda(1) + \max\left(\frac{\lambda(1)}{r}, c\right)$.
- Free-riders win: $(0, 1 - cr, 0)$. This state is stable if $\frac{1}{r} > \max(a, c)$.
- Isolated coexistence point (always unstable):

$$\left(G^* \left(1 - \frac{c(r-1)}{1-a}\right), (1 - G^*) \left(1 - \frac{c(r-1)}{1-a}\right), G^*\right), \qquad (1)$$

  where

$$G^* = \frac{1}{\beta}\left[\sigma - \ln\left(\frac{(1 + e^\sigma)(r-1)}{r(1-a)} - 1\right)\right]$$

- Non-isolated coexistence line: $(G^*, 1 - G^*, G^*)$. At least some finite part of this interval containing $G^* = 0$ is stable.

public good evolutionary games among cancer cells, collective benefit (at individual cost?)

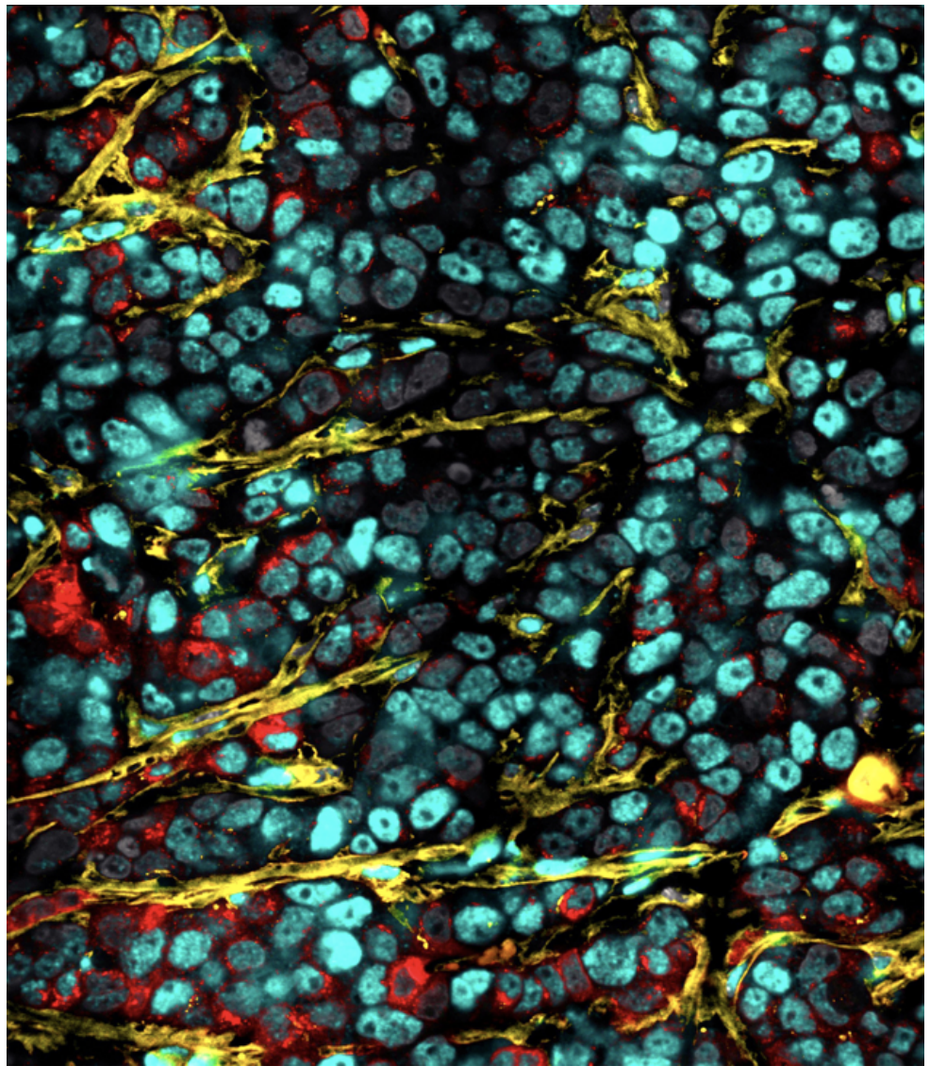

Image credit: Doris Tabassum
In heterogeneous MDA-MB-468 xenografts, IL11+ cells (secreted IL11 in red) act as non-cell autonomous driver of tumor growth by influencing pSTAT3 signaling (cyan) in the neighboring carcinoma and stromal (yellow) cells; nuclei are marked in grey. (Montage of 6 images on a 60X objective).